Poly (glycolic acid) (PGA): a versatile building block expanding high performance and sustainable bioplastic applications

Paresh Kumar Samantaray[1], Alastair Little[1], David M Haddleton[2], Tony McNally[1], Bowen Tan[3], Zhaoyang Sun[3], Weijie Huang[3], Yang Ji[3], Chaoying Wan[1]*

[1] *International Institute for Nanocomposites Manufacturing (IINM), WMG, University of Warwick, CV4 7AL, U.K.*

[2] *Department of Chemistry, University of Warwick, CV4 7AL, UK*

[3] *PJIM Polymer Scientific Co., Ltd., Shanghai, 201102, China*

* Email: Chaoying.Wan@warwick.ac.uk

ABSTRACT

The concerns about the accumulating plastic waste pollution have stimulated the rapid development of bioplastics, in particular biodegradable bioplastics derived from renewable resources. Driven by a low carbon circular economy, bioplastics production is estimated to reach a 40 % share of the plastics market by 2030 (Bioplastics Market Data, 2018). It is expected to substitute petrochemical-based plastics in many applications, from food packaging, pharmaceuticals, electronics, agriculture to textiles. The current biodegradable bioplastics have met challenges in competing with engineering polymers such as PET and Nylon in terms of processing capacity at industry scale, mechanical robustness, thermal resistance, and stability. Poly (glycolic acid) (PGA) has a similar chemical structure to PLA but without the methyl side group, which allows the polymer chains to pack together tightly and results in high degree of crystallinity (45~55%), high thermal stability (T_m =220~230 °C), exceptionally high gas barrier (3 times higher than EVOH), as well as high mechanical strength (115 MPa) and stiffness (7 GPa). Meanwhile, PGA is rapidly biodegradable and 100% compostable, showing a similar biodegradation profile to cellulose. To date, PGA has been mainly used in the form of copolymers, such as poly(lactic-*co*-glycolic acid) (PLGA). Its unique properties have often been overlooked and are yet to be explored. This is caused by its intrinsic characteristics such as high hydrophilicity, rapid degradation, insolubility in most organic solvents and brittleness that have hindered its practical applications. Here we introduced the synthetic chemistry, processing methods, modification, and applications of PGA, aiming to provide a critical discussion about the technical challenges, development opportunities, and solutions for PGA-based materials. The future direction and perspectives for high-performance PGA are proposed. Given its synthesis diversity and unique properties, PGA shows great potential to substitute engineering petrochemical-based polymers for high temperature and high gas barrier packaging applications.

View Article Online
DOI: 10.1039/D0GC01394C

1. Introduction

Limited fossil fuel resources, increased waste disposal problems, and accumulation of non-biodegradable plastic waste have become significant concerns to the environment and threats towards sustainable eco-systems. Since the 1950s, an estimate of nearly 6.3 billion tonnes of plastic waste has been produced worldwide, of which only 9 % are recycled and another 12 % incinerated. In contrast, 79% of the waste was accumulated in landfills or the natural environment.[1] Disposal of plastic solid wastes by landfill and incineration has resulted in increasing carbon dioxide (CO_2) emissions, which in turn leads to global warming.[2] Conventional petrochemical-based synthetic polymers are one of the main contributors to plastic waste, such as polyolefins (polyethylene, polypropylene), polyethylene terephthalate (PET), Nylon as well as their blends and composites. A sustainable step towards a low carbon footprint can be targeted by developing biodegradable, and bio-mass derived plastics to replace non-biodegradable and petrochemical-based plastics.

Bioplastics are defined as those polymers which are derived from renewable sources, biological systems (bio-based), and/or are biodegradable as per European Bioplastics, a European association representing the interests of the bioplastics industry along the entire value chain. [3] Figure 1 shows the classification of bioplastics based on their sources of origin. It can be noted that biodegradable polymer is a sub-set of bioplastics, and not all bioplastics are biodegradable. As per ASTM D6813, "Biodegradable" is defined as "Capable of undergoing decomposition into CO_2, methane, water, inorganic compounds, or biomass in which the predominant mechanism is the enzymatic action of microorganisms, that can be measured by standard tests, in a specified period, reflecting available disposal condition."[4] Similarly, the International Union of Pure and Applied Chemistry (IUPAC) defines a biodegradable polymer as a "polymer susceptible to degradation by biological activity, with the degradation accompanied by a lowering of its molar mass."[5] Essentially, during biodegradation, long macromolecular chains are broken down *in-vitro* or *in-vivo* by enzymes (and other biologically active entities) into shorter chains, which are further metabolized by microorganisms. In essence, biodegradable polymers should break down cleanly, in a defined time, to simple molecules found in the environment such as CO_2 and water under enzymatic action. Poly (glycolic acid) (PGA) and its copolymers undergo biodegradation via chemical hydrolysis rather than enzymatic hydrolysis, so biodegrade even in the absence of enzymes. This results in PGA having much faster rates of biodegradation than other common biodegradable polyesters such as polycaprolactone (PCL) and polybutylene adipate-co-terephthalate (PBAT).

The latest report of European Bioplastics, Nova institute 2019, estimates the current bioplastics production at 2.11 million tonnes and projects that it will increase up to 2.42 million tonnes by 2024.[6] As per the same report, packaging (rigid packaging, flexible packaging, and consumer goods) remains the largest market segment for bioplastics with more than 53 percent (1.14 million tonnes) of the total bioplastics market in 2019.[6] Biodegradable polyesters play a crucial role in the degradable segment of bioplastics with poly(lactic acid) (PLA) leading usage. Although PLA manifests excellent mechanical

View Article Online
DOI: 10.1039/D0GC01394C

properties, transparency, melt-processing ability, slow degradation rate, its low thermal stability, and acidic degradation of its derivatives have limited its applications in food packaging, textile, and medical sector. Further, considering the diverse range of challenging applications of biodegradable bioplastics, the search for a new material analog of PLA with better performance characteristics has started.

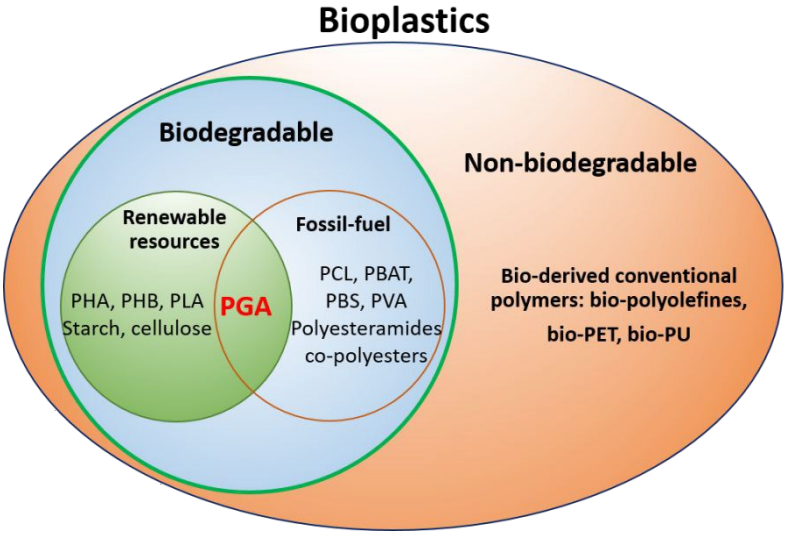

Figure 1: Classification of bioplastics, where PGA can be made from either biomass or fossil-based natural gas.

PGA has a similar structure to PLA but possesses higher heat distortion temperature, excellent mechanical, in particular, exceptionally higher gas barrier properties.[7] New technological interventions on the industrial-scale have paved the way towards the commercial availability of this polymer. Its consumption among the biodegradable market shows an annual growth rate of 10 %, the global market for PGA was estimated at around 182 million USD in 2014, which rose to 240 million USD in 2017, and it is expected to increase to 470 million USD by 2024.[7] The oil and gas industry and packaging are some of the key areas where its application and prospects are much sought after owing to its exceptional mechanical robustness, thermal stability, chemical resistance, and gas barrier properties, comparable to engineering polymers such as PET, PPO and Nylon 6.

Currently, glycolic acid, a monomer of PGA, is mainly utilized as a co-monomer to synthesize poly(lactic-co-glycolic acid) (PLGA) copolymers, to balance the mechanical strength and biodegradability of PLA. PLGA copolymers are a family of Food and Drug Administration (FDA) approved biodegradable polymers mainly used in biomedical applications such as sutures, prosthetic devices, or drug delivery vesicles. The exploitation of PGA-based copolymers in the areas of shape memory films, antibacterial coatings, food packaging products, and biomedical scaffolds will provide more opportunities for developing high performance and functional green plastic products.

This review highlights the potential of PGA in generating a broad range of biodegradable polymers for a variety of applications, given its diverse synthetic chemistry, high thermal stability, high gas barrier, high mechanical strength, fast biodegradation and compostability. The synthesis of high molecular weight PGA homopolymers and copolymers, and characteristic properties in terms of conformation, crystallization, and degradation are critically reviewed. Their application in tissue engineering, drug delivery, packaging, sensing, and thermal management are discussed. The future potential and prospects for PGA based biodegradable polymers are highlighted.

2. Synthesis of PGA and PGA based copolymers

2.1 PGA polymerization

PGA can be synthesized via different chemical routes. The simplest of which is the direct poly-condensation polymerization of glycolic acid. However, this generally yields M_n lower than 50,000 g mol^{-1}. To achieve higher molecular weight, ring-opening polymerization (ROP) of glycolide, the cyclic dimer of glycolic acid is generally used. Alternatively, PGA can also be synthesized via solid-state polycondensation (SSP) of halogen acetates or by reacting formaldehyde (trioxane) with carbon monoxide (CO). The current industrial route towards PGA is through the ROP of glycolide.[8]

Despite its excellent properties, PGA production is low due to limitations in monomer (glycolic acid or glycolide) production and high price. Glycolic acid can be produced via hydrolysis of chloroacetic acid, which is highly corrosive and toxic. This route faces issues with product quality (impurities) and scale-up. Currently, glycolic acid is predominantly produced from the carbonylation of formaldehyde, requiring high temperatures and pressures. Formaldehyde may also be converted into glycolonitrile, which is then converted into highly pure glycolic acid via an enzymatic process. As Figure 2 shows, these routes all share methanol as a starting material. Methanol is typically produced from syngas (CO and H_2) obtained from fossil-based natural gas. Methanol and syngas (CO and H_2) can also be obtained from biomass (wood distillation, biomass gasification, and fermentation), although these processes are less economical.[9,10] Additionally, electrochemical routes towards both methanol and glycolic acid also exist via the electrocatalytic reduction of CO_2 into formate.[11]

A new process from syngas to PGA was recently developed by Pujing Chemical Industry Limited Co. Ltd (PJCHEM), China. The chemical process is shown in Figure 2 (middle line). In this process, firstly, syngas is purified and separated into CO and H_2. Then methanol, CO, and O_2 are used to produce dimethyl oxalate (DMO) by esterification and carbonylation. The monomers methyl glycolate (MG) or GA are produced from DMO by hydrogenation or hydrolysis. PGA is then obtained from MG or GA. This new process is advantageous due to its ease of scale-up and high monomer purity, unlike in traditional routes, the monomer contains no Cl or HCN impurities—these are detrimental to polymerization and require removal. Additionally, the process can be considered to be more environment friendly, since it avoids the use of toxic chemicals and utilises CO from coal industry waste gases, previously such gases would have been burnt into CO_2, contributing to the greenhouse

View Article Online
DOI: 10.1039/D0GC01394C

effect. In 2017, PJCHEM constructed a plant with a capacity of 10 Kilo tonnes per year in Inner Mongolia. P.R. China and a new plant with a production capacity of 50 Kilo tonnes per year in Shanxi Province. P.R China in 2020.[12, 13]

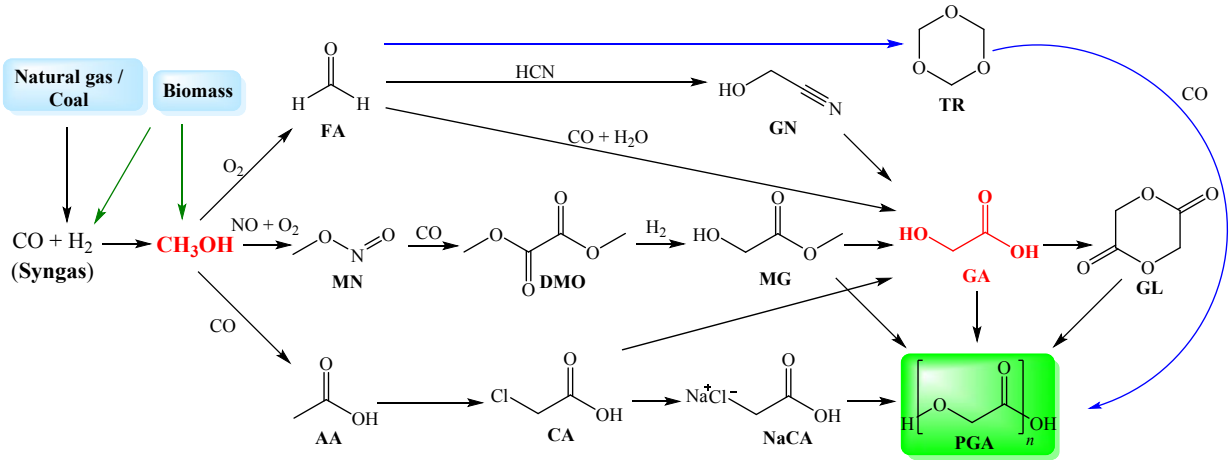

Figure 2: A summary of the synthetic routes towards PGA. FA = formaldehyde, GN = glycolonitrile, TR = trioxane MN = methyl nitrite, DMO = dimethyl oxalate, MG = methyl glycolate, GA = glycolic acid, GL = glycolide, AA = acetic acid, CA = chloroacetic acid, NaCA = sodium chloroacetate, PGA = poly (glycolic acid)

2.1.1 Ring-Opening Polymerization of Glycolide

The ROP of glycolide produces PGA with high molecular weights (M_n > 100,000 g mol^{-1}) and high conversions. It also enables control of molecular weight by altering initiator concentration. The only disadvantage of ROP is that it requires glycolic acid to be converted into glycolide, increasing the energy demands and costs of the process. The high cost of glycolide production has limited the application of PGA. To obtain glycolide, glycolic acid is heated under reduced pressure in the presence of a catalyst to form PGA oligomers. Further heating these oligomers under reduced pressure produces glycolide, which is removed via distillation.[14] The resulting glycolide requires further purification to remove traces of water and glycolic acid; these terminate chains in ROP, lowering molecular weight. Figure 3 compares the direct polycondensation process with the ring-opening polymerization.

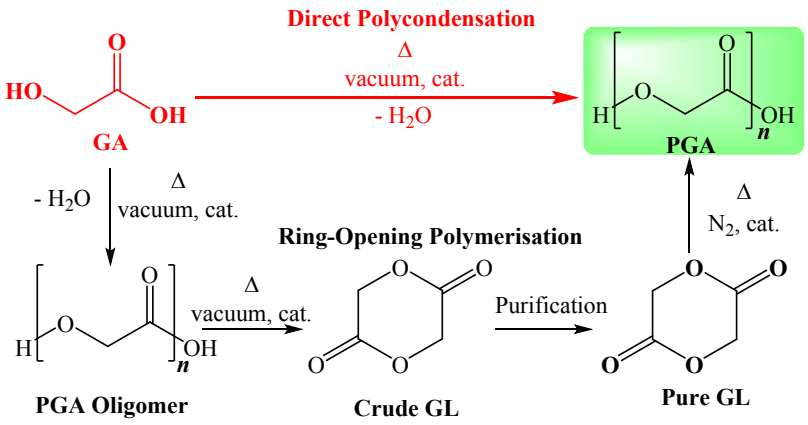

Figure 3: Comparison of the routes to PGA via direct polycondensation and ring-opening polymerization (ROP).

The ROP of glycolide is performed in bulk via batch processes at 150~230 °C for 2~6 h using tin (II) catalysts under inert (N_2) conditions, 1-dodecanol is often added as an initiator. The reaction has fast reaction kinetics. When using $Sn(Oct)_2$ at 220 °C, the reaction reaches an 80% conversion after 30 minutes, increasing to 96 % after 4 hours.[14] A variety of reaction conditions and the resulting molecular weights have been reported and are summarised in Table 1.

Generally, the reaction mixture is heated to a temperature between the melting point of glycolide and PGA. As the reaction progresses, melt viscosity increases, creating stirring difficulties and reduced heat transfer; this generates a heterogeneous polymer mixture. This increase in viscosity also makes it difficult to remove the product from the reactor. To enable more efficient heat transfer, the mixture is often heated above the melting or softening point of PGA (220~230 °C) to induce melt polymerization. However, such high temperatures encourage depolymerization reactions such as intermolecular and intramolecular transesterification (backbiting), which lower the molecular weight and cause discoloration of the PGA (white to brown).[15] Kureha Corporation Japan, the global leaders in PGA production, manufacture PGA by beginning the polymerization in the melt state and continuing in the solid-state (150~200 °C) after a sufficient conversion is reached, achieving a high molecular weight with little discoloration.[8] Following polymerization, the resulting polymer is often crushed, washed with solvent (ethyl acetate or acetone) and vacuum dried to remove residual glycolide.[16, 17]

Supercritical CO_2 ($ScCO_2$) has also been used to lower the reaction temperature and avoid thermal degradation. Using $ScCO_2$, Schmidt et al. synthesized white PGA with an M_n of 31,000 g mol^{-1} and low polydispersity (1.3) at 120 °C.[18] Bratton et al. also used $ScCO_2$ to synthesize PGA at 80 °C, low M_ns (4,200~4,900 g mol^{-1}) was achieved.[19]

Table 1. Reaction conditions used for the ROP of glycolide

Method	Temp / °C	Time / h	Catalyst	Initiator	Molecular Weight / g mol^{-1}
Bulk ROP[20]	230	30 min	$Sn(Oct)_2$ (0.002mol%)	1-dodecanol	M_n > 45,000
Bulk ROP[14]	220	4	$Sn(Oct)_2$ (0.03 mol%)	1-dodecanol (0.01 mol %)	M_n 25,000-40,000 M_w 60,000-90,000
Bulk ROP[17, 21]	180	4	$SnCl_2{\cdot}2H_2O$ (0.003 mol %)	none	M_w 250,000 Đ 2.7
Bulk ROP[17, 21]	200, 160	3, 12	$SnCl_4$ (0.002 mol %)	1-dodecanol (0.003 mol %)	M_w 238,000 Đ 1.7
Bulk ROP[17, 21]	〃	〃	〃	1-dodecanol (0.030 mol %)	M_w 110,000 Đ 1.9
Bulk ROP[16]	140	20 min	Ph_2BiBr (0.13 mol %)	none	M_n 245,000
ROP in	RT	1	TBD (1 mol %)	None	M_p 19,800

acetonitrile[22]					Đ 2.3
	-20	1	DBU (1 mol %)	None	M_p 31,900 Đ 2.0
ROP in $ScCO_2$[18]	120	5	$Sn(Oct)_2$ (0.003 mol %)	1-dodecanol (0.02 mol %)	M_n 31,200 Đ 1.3

An initiator containing hydroxyl groups, such as 1-dodecanol, is often added to the reaction to accelerate the polymerization and control molecular weight via the formation of unreactive end groups. Decreasing the initiator concentration increases the molecular weight. The initiator coordinates to the tin (II) catalyst to generate a tin alkoxide of greater nucleophilicity, which acts as the true initiating species. The tin alkoxide then ring opens the glycolide via nucleophilic attack, and polymerization proceeds through a coordination insertion mechanism (Figure 4). Impurities such as water and glycolic acid also act as initiators. [23]

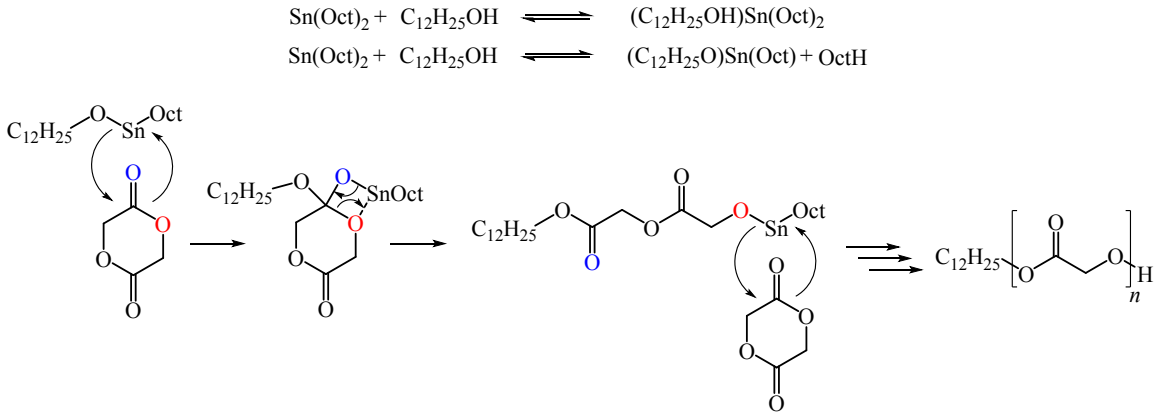

Figure 4: Coordination-insertion mechanism for ROP of glycolide catalyzed by $Sn(Oct)_2$ using 1-dodecanol as an initiator

The initiator also determines the polymer end group, affecting the physical and chemical properties of the polymer. By substituting 1-dodecanol for 1,4-butanediol, Gautier et al. raised the T_g of PGA from 25 °C to 36 °C and lowered the T_c from 181 °C to 151 °C, and both polymers were of similar molecular weights (Table 2).[20]

Table 2. PGA synthesized using 1-dodecanol as initiator vs. using 1,4-butanediol as initiator.[20]

Initiator	PGA Structure	T_g / °C	T_m / °C	T_c / °C
1-dodecanol	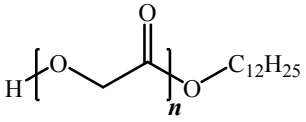	25	224	181
1,4-butanediol	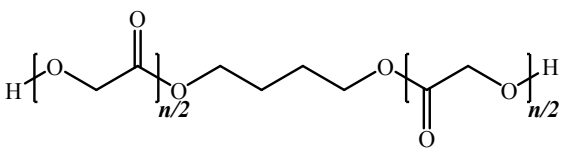	36	222	151

Due to its high activity and acceptance as an FDA approved food additive, tin(II) bis(2- ethyl hexanoate) ($Sn(Oct)_2$) is the most commonly used catalyst for the ROP of lactones. $Sn(Oct)_2$ catalyzes ROP via a coordination-insertion mechanism (Figure 4). However, concerns are surrounding the cytotoxicity of tin compounds. Tin catalysts also catalyze transesterification side reactions at higher temperatures, broadening molecular weight distributions. Thus many alternatives, non-toxic catalysts with potentially higher selectivity towards ring-opening have been investigated.[23,24]

Lu et al. used non-toxic diphenyl bismuth bromide (Ph_2BiBr) to synthesize very high molecular weight PGA (M_n 20,000-250,000 g mol^{-1}) at low reaction temperatures (120~150 ^oC) and short reaction times (< 30 minutes). A white PGA was formed, indicating a lack of degradation and side reactions.[16] Various non-toxic organocatalysts have also been successfully used to synthesize PGA.[22] Kemo et al. used the organocatalysts 1,8-diazabicyclo[5.4.0]undec-7-ene (DBU), 1,5-diazabicyclo[4.3.0]non-5-ene (DBN) and 1,5,7- triazabicyclo[4.4.0]dec-5-ene (TBD) at low temperatures (-20 to RT ^oC) to synthesize PGA in solution (acetonitrile) in one hour. Although the final polymer was white, the reaction conversions (17~42%) and molecular weights obtained were relatively low (M_p = 12,200 ~ 31,900 g mol^{-1}).

2.1.2 Polycondensation from glycolic acid

PGA can also be obtained directly from glycolic acid through polycondensation polymerization. This occurs via esterification reactions, eliminating water, typically removed using a vacuum to push the equilibrium towards the product (Figure 5). This becomes difficult as the viscosity of the mixture increases, making it hard to achieve high molecular weights. These reactions require high temperatures, high vacuums, and prolonged reaction times, and such conditions encourage depolymerization reactions forming glycolide (Figure 5), further limiting the molecular weight obtained. These conditions also promote transesterification reactions and discoloration. Despite these problems, melt/solid-state polycondensation and azeotropic polycondensation have been used to synthesize PGA of fairly high molecular weights (Table 3).

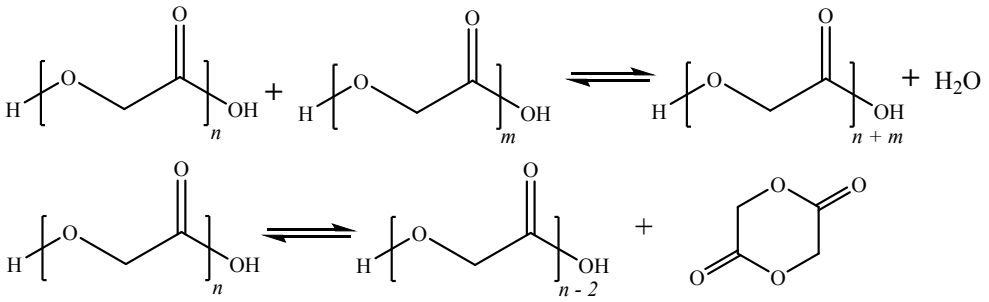

Figure 5: The equilibria present in the polycondensation of glycolic acid

View Article Online
DOI: 10.1039/D0GC01394C

Takashi et al. polymerized glycolic acid via melt-polycondensation (190 °C, 5 h, vacuum) followed by solid-state polymerization at the same temperature for 20 hours to achieve brown PGA with an M_n of 45,000 g mol^{-1} and an M_w of 91,000 g mol^{-1} using zinc acetate dihydrate ($Zn(CH_3CO_2)_2 \cdot 2H_2O$) as a catalyst.

Solution-based polycondensation can be used to lower the reaction temperature and reduce depolymerization reactions. However, due to the poor solubility of PGA, this has seldom been performed. Ayoob et al. prepared white PGA via solution polycondensation in diphenylsulfone at 170~190 °C under vacuum over 24 hours using methane sulfonic acid (MSA) as a catalyst. Molecular weights were not measured directly; however, the resulting PGA had a similar inherent viscosity to commercial Kuredex samples, suggesting high molecular weight.[25] Using solvents that form azeotropes with water, solution-based polycondensation can be performed where water is removed via azeotropic distillation. Sanko et al. synthesized PGA of M_n of 27,000 g mol^{-1} via azeotropic polycondensation at 154 °C over 30 hours using anisole as the solvent and triflic acid (TfOH) as the catalyst.[26]

These polymerization techniques all require significantly longer reaction times as well as high catalyst concentrations. Thus, the resulting polymers will contain more catalyst impurities. Although fairly high molecular weights can be achieved via polycondensation, they are still well below those achievable via ROP.

2.1.3 Other Synthetic Routes

PGA can also be synthesized directly from formaldehyde and carbon monoxide (Figure 2). Such a route appears attractive as it reduces the number of reaction steps, removing the need for the energy-intensive production of glycolide. Göktürk et al. used trioxane (an anhydrous source of formaldehyde) to synthesize low molecular weight PGA using triflic acid as a catalyst, this was then subjected to post-polymerization catalyzed by zinc acetate dehydrate to achieve high molecular weight PGA (M_n >45,000 g mol^{-1}). In total, the reaction took 86 hours, was performed at 170-200 °C, and required the use of a high vacuum for long periods. Thus, it does not appear to be a significantly more energy-efficient route than the ROP of glycolide.[9]

Upon heating, metal halides are eliminated from halogenoacetates; this forms PGA. Low molecular weight PGA (2,300 g mol^{-1}) was synthesized by Schwarz et al. by heating sodium chloroacetate (NaCA) at 160 °C under nitrogen for 1000 minutes in the absence of a catalyst. NaCl was formed alongside the PGA, which can be removed via washing with water, yielding a porous polymer.[27] Table 3 shows the experimental conditions for producing PGA using other chemical routes.

View Article Online
DOI: 10.1039/D0GC01394C

Table 3. Conditions used for polycondensation processes and other methods to produce PGA

Method	Temp / °C	Atmosphere	Time / h	Catalyst	Solvent	Molecular Weight / g mol $^{-1}$	T_m / °C
Melt PC[28]	190	1) 150-30 mm Hg 2) N_2	1) 5 2) 20	$Zn(OAc)_2 \cdot 2H_2O$ (0.26 mol %)	-	M_n 45,000 M_w 91,000	220
Solution PC[25]	170-190	50 torr	24	MSA (0.6 mol %)	Diphenyl sulfone		229
Azeotropic PC[26]	154	Ar	30	TfOH (1 mol %)	Anisole	M_n 32,100 M_w 40,300	218
Trioxane + CO[9]	1) 170 2) 200	1) 800 psi CO 2)150 mm Hg	1) 72 2) 2,12	1) TfOH (1 mol %) 2) $Zn(OAc)_2 \cdot 2H_2O$ (0.26 mol %)	DCM	M_n > 45,000	219
SSP of sodium chloroacetate[27]	180	N_2	10	None	-	M_n 2,300	

2.2 PGA based copolymers

There are four key challenges associated with PGA homopolymers,

1) The degradation temperature (T_d ~250 °C) is close to T_m (220 ~ 230 °C), making it hard to process without causing thermal degradation. Its heat resistance can be improved by adding compounds that deactivate the residual catalyst.[8]
2) It has a rapid hydrolysis rate, causing the material to biodegrade very quickly, making it inapplicable for any long-term applications. Yamane et al. slowed the hydrolysis rate of PGA by order of magnitude by altering the end-group structure with hydrolysis stabilizers (such as N, N-2,6-diisopropylphenylcarbodiimide) and reducing the amount of residual glycolide present. [29]
3) It is insoluble in most organic solvents. At room temperature PGA will only dissolve in fluorinated solvents such as HFIP, making characterization very expensive.
4) Although it has excellent mechanical properties, it has a low extension at the break, making it brittle and unsuitable for many applications.

These issues are overcome using copolymerization. Figure 6 provides an overview of different co-monomers for synthesis PGA based copolymers. Lactide, ε-caprolactone, trimethylene carbonate, and p-dioxanone have all been successfully copolymerized with glycolide to produce copolymers for biomedical applications, such as biodegradable sutures, drug delivery devices, scaffolds, implants and tissue engineering.[30, 31] Variation of the co-monomer composition allows the mechanical properties and degradation kinetics of these materials to be tailored specifically for the required use. Such copolymers are typically synthesized via ROP using tin catalysts under conditions similar to those used for PGA (Figure 8).

View Article Online
DOI: 10.1039/D0GC01394C

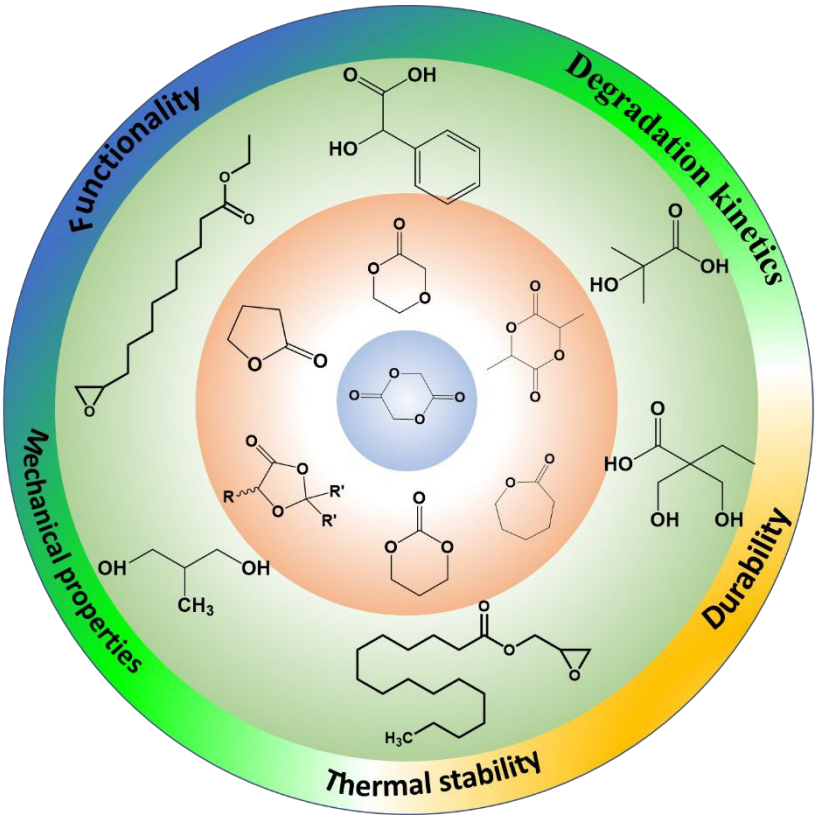

Figure 6: Overview of co-monomers used for the synthesis of PGA based copolymers, and the potential to tuning the mechanical, thermal, functionality, and degradation properties of the copolymers.

2.2.1 PLGA - Poly(lactic acid-co-glycolic acid)

PLGA is the most common bioresorbable copolymer. It is a rigid, brittle material with a T_g of 30 ~ 60 °C. It is usually synthesized in high molecular weights via the ROP of lactide and glycolide using tin catalysts (Figure 8). Lactide is the cyclic dimer of lactic acid, a bio-based α-hydroxy acid produced via sugar fermentation. Lactic acid's methyl group makes PLA a more hydrophobic material than PGA, as a result, it takes longer to biodegrade. A wide range of properties can be obtained by adjustment of the following factors,

1) **The LA:GA ratio.** Increasing the GA content increases hydrophilicity. Thus, as the GA content is increased from 0 to 50 mol %, the rate of hydrolysis/biodegradation increases.[32] However, the crystallinity is also altered as the copolymer composition changes, so as the GA content is further increased to 100 mol %, the rate of hydrolysis/biodegradation reduces. Thus, PLGA50 (50:50 LA:GA) degrades the fastest.[14]

2) **The lactide stereo-isomeric composition (D-, L- or D,L-lactide).** D,L-lactide produces amorphous copolymers with faster degradation rates. Copolymers of L-lactide are semi-crystalline and more brittle.
3) **The monomer sequence (sequenced or random).** Sequenced PLGA copolymers have a slower degradation rate than random PLGA copolymers.[33]
4) **Molecular weight.** Increasing the molecular weight increases the degradation time and improves thermomechanical properties.[34] When the M_n of PLGA75 was increased from 3,400 g mol^{-1} to 99,000 g mol^{-1} its T_g increased from 22 ^{o}C to 51 ^{o}C.[35]
5) **End-group.** PLGA with ester end-groups takes longer to degrade than PLGA with carboxylic acid end-groups.[34]

2.2.2 PGC - Poly(glycolic acid-co-ε-caprolactone)

ε-caprolactone is a fossil-derived monomer used to make biodegradable polymers with higher elasticity and slower biodegradation rates than PGA. PGC copolymers are rubbery with longer degradation times than PGA. Like PLGA, the material properties and degradation rate can be controlled by varying the monomer ratios and the chain microstructures, some of these properties are shown in table 4. Because glycolide has a greater reactivity than ε-caprolactone, random PGC copolymers tend to contain large PGA blocks. Lee et al. synthesized random PGC (50:50) via ROP (170 ^{o}C, 20 hours, $Sn(Oct)_2$) and compared it to PLGA (70:30 L:G). The PGC showed a lower T_g, greater elongation at break, lower tensile strength and higher recovery from stress-induced deformation than the PLGA.[36]

Monocryl is a bioabsorbable suture made from segmented PGA-PGC block copolymers consisting of a 75:25 GA: ε-CL molar ratio. Figure 7 outlines its synthesis, glycolide (45 mol %), and ε-caprolactone (55 mol %) undergo ROP (190 ^{o}C, 17 hours, $Sn(Oct)_2$) using diethylene glycol as an initiator to produce PGC chains with hydroxyl end groups. These are then reacted with glycolide (230 ~ 200 ^{o}C, 2 hours) to create a PGA-PGC-PGA block copolymer.[37] In this reaction, PGC acts as a macrodiol initiator. Macrodiols are synthesized by the ROP of monomers in the presence of diols as initiators, homopolymer-diols, or copolymer-diols can be formed. Using these macroinitiators for ROP allows block copolymers with more ordered structures to be produced to control material properties.

Cai et al. synthesized PEG-PGC-PEG ABA triblock copolymers via the ROP of glycolide and caprolactone using PEG as an initiator. By introducing PEG, the hydrophilicity of the copolymer was increased, and the degradation time and tensile strength were reduced.[38]

View Article Online
DOI: 10.1039/D0GC01394C

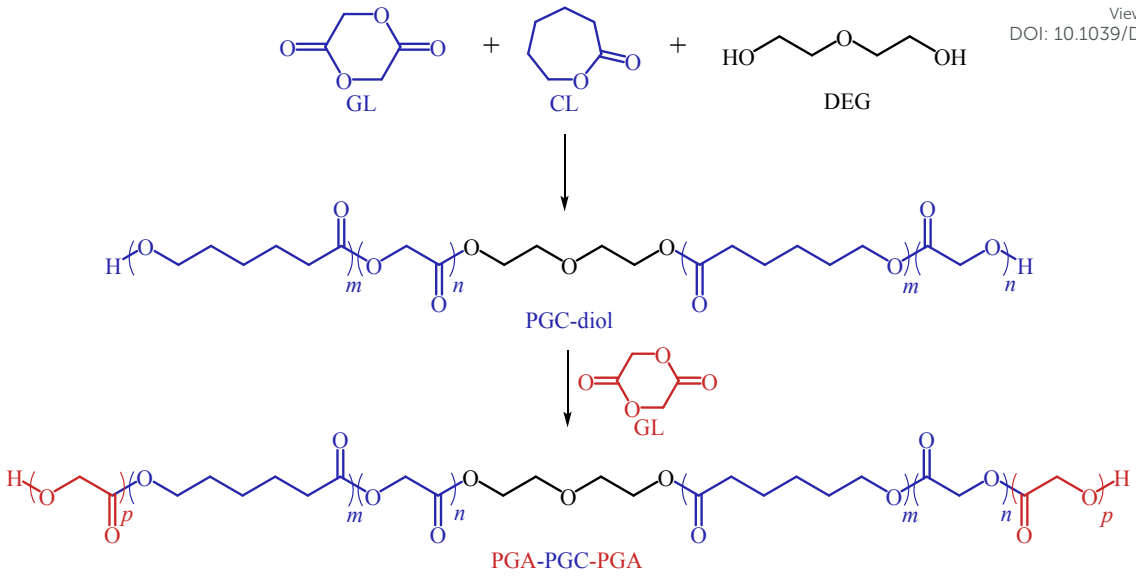

Figure 7: Synthesis of PGA-PGC-PGA block copolymer (monocryl). GL= glycolide, CL= ε-caprolactone, DEG = diethylene glycol, PGA-PGC-PGA = poly(glycolic-acid-block-(glycolic acid-co-ε-caprolactone)-block-glycolic acid)

2.2.3 PGTMC - Poly(glycolic acid-co-trimethylene carbonate)

Like ε-caprolactone, trimethylene carbonate can be used to lower the T_g of PGA. PGTMC is more elastic and more hydrophobic than PGA; it also has a longer degradation time.[39] Maxon is a bioresorbable suture containing a 67.5:32.5 GA:TMC molar ratio. It is a PGA-PGTMC-PGA block copolymer synthesized in a similar way to Monocryl (Figure 7). [40]

Table 4. Properties of PGA-copolymers

Copolymer	GA % / mol %	M_n / g mol^{-1}	Đ	T_g / °C	σ / MPa	E / MPa	ε_b / %	Biodegradation / Weight loss after time
L-PLGA								
RESOMER® LG855S	15	-	-	58	80~ 90	3,500~ 4,500	<10	1-2 years
[41]	15	70,000	1.9	54	49	2,200	1.1	-
[36]	30	132,000	2.2	56	-	-	20	-
[41]	50	154,000 (M_v)	-	42	39	3,320	1.9	-
[41]	80	119,000 (M_v)	-	39	36	3,690	1.1	-
D, L-PLGA								
[42]	15	-	-	50~55[11]	41~ 55[42]	1,400~ 2,800 [42]	3~10[42]	5~6 months
[42]	25	-	-	38~50[11]	″	″	″	4~5 months
[42]	50	-	-	30~35[11]	″	″	″	1~2 months
[43]	50	-	-	44	51.6	3,140	37.9	100 %, 7 weeks

View Article Online
DOI: 10.1039/D0GC01394C

[44]	24	242,000	2.4	58	46.1	670	10~20	-
PGC								
[38]	20	68,200	1.9	-63	32.9	-	-	34 %, 55 weeks
[36]	50	121,000	1.6	-19	~0.6	-	>250	50 %, 6 weeks
[45]	50	57,000	2.0	-16	5.13	0.007	653	75 %, 12 weeks
PGTMC								
[46]	28-89	10,800~ 22,300	1.9-2.7	-8~31	-	-	-	-
[47]	67.5	45,600	1.8	21	33	202	615	30 %, 7 weeks
PGA-PTMC-PGA[47]	67.5	34,000	1.5	-12	36	659	23	17 %, 6 weeks
PGA-PGTMC-PGA[47]	67.5	38,200	1.7	20	36	377	287	18 %, 6 weeks

GA % = glycolic acid % of the copolymer, σ = Tensile strength, E = Young's Modulus, ε_b = Elongation at break. All biodegradation studies were carried out at 37 °C in a phosphate buffer solution of pH 7.4.

Random PGTMC copolymers, PGA-PGTMC-PGA segmented copolymers, and PGA-PTMC-PGA triblock copolymers were synthesized by Diaz-Celorio et al. The random PGTMC copolymer showed the fastest degradation rate, introducing PGA end segments reduced this rate. Increasing the amount of GA in the middle PGTMC segment increased the degradation rate. The random PGTMC copolymer was the most elastic, and the PGA-PTMC-PGA triblock copolymer was the least flexible and showed the slowest degradation rate (Table 4). Thus the material properties and rate of hydrolytic degradation can be actively controlled by the microstructure (random, triblock or segmented).[47]

Because PLGA is rigid and brittle, ε-caprolactone or trimethylene carbonate are often added to engineer a more pliable and elastic polymer. The resulting terpolymers, PLGC and PLGT show rubber-like mechanical properties and are softer and more flexible than PLGA. Poly(ethylene glycol) (PEG) has also been introduced into PLGA to produce a variety of commercially available diblock and triblock terpolymers.

2.2.4 PLGC- (Poly(lactic acid-glycolic acid-co-ε-caprolactone)

PGLC terpolymers are synthesized via ROP using similar conditions to those used for PGA and PLGA (Figure 8). However, longer reaction times (up to 48 h) are required due to the lower reactivity of ε-caprolactone in comparison to glycolide and lactide (GA>LA>CL).[48] Random PLGC terpolymers show increased elongation at break and reduced T_g in comparison to PLGA.[48] Table 5 lists the properties of various PLGC terpolymers, incorporating more ε-caprolactone into the polymer reduces the T_g, tensile strength and Young's modulus. Degradation studies have shown that the glycolic acid units degrade the quickest. In contrast, the ε-caprolactone units degrade the slowest, and the overall hydrolysis rate is impacted significantly by the monomer ratios. [45, 48]

View Article Online
DOI: 10.1039/D0GC01394C

Various block copolymers such as ABA PLGA-PCL-PLGA tri-block terpolymers have also been produced, PLGA-PCL-PLGA is synthesized from lactide, glycolide and PCL-diol (Figure 8).[49] PLA-PGC multiblock copolymers were prepared by Min et al. by coupling PLA-diols and PGC-diols (G:C 1:2) using 1,6-hexanediisocyanate as a coupling agent. The M_n of the macrodiols was varied from 2,000~10,000 g mol^{-1}. All terpolymers had M_ns between 90,000~120,000 g mol^{-1} and elongations at break greater than 300 %. Increasing the M_n of the macrodiols increased the terpolymers' thermal properties (T_g and T_m), crystallinity, and tensile strength while decreasing their elongation at break. Degradation time was also increased by using macrodiols of a higher M_n. For a PLLA:PGC ratio of 60:40, as the macrodiols' M_n, was increased from 2000 to 10,000 g mol^{-1}, the copolymers T_g increased from 40 °C to 47 °C, and T_m increased from 136 °C to 158 °C. Increasing the PGC content also increased the elongation at break, changing the material from hard to rubbery.[50] PLGC block copolymers generally show higher T_g, higher tensile strength, and longer biodegradation times than random PLGC (Table 5).

2.2.5 PLGT - (Poly(lactic acid-glycolic acid-co-trimethylene carbonate)

Much research has also been performed into the development of PLGT as a bioresorbable material.[51-53] By adjusting the monomer ratios, the mechanical properties of PLGT can be tuned from being rigid to rubber-like Zini et al. synthesized a range of random PLGT terpolymers of a variety of compositions, incorporating more trimethylene carbonate generally reduced the T_g, tensile strength and Young's modulus of PLGT (Table 5). These polymers showed high shape recovery after deformation. Using $Zr(Acac)_4$ as a catalyst was shown to improve their thermal stability in comparison to those synthesized with $Sn(Oct)_2$. [53]

PLGA-PTMC-PLGA block terpolymers have also been explored.[54] Smola et al. synthesized these using branched PTMC macroinitiators of various M_ns. Branching was introduced into the PTMC macrodiols by using initiators with varying amounts of hydroxyl groups to synthesize them. Using glycerol or pentaerythritol as initiators created cross-linked PTMC oligomers, which, when used as macroinitiators, introduced small amounts of cross-linking into the terpolymer, improving the mechanical properties.[51] Table 5 shows the thermo-mechanical properties of PLGA-terpolymers, while Figure 8 summarizes the common routes adopted for designing glycolic acid copolymers.

Table 5. Properties of PLGA-terpolymers

Copolymer	Monomer Ratio / mol %	M_n / g mol^{-1}	Đ	T_g / °C	σ / MPa	E / MPa	ε_b / %	Biodegradation / Weight loss, weeks after
PLGC	L:G:C							
L-PLGC								

[45]	10:40:50	78,000	2.1	-14	0.014	0.00005	561	90 %, 12
[45]	20:30:50	84,000	1.8	-10	0.034	0.00014	555	70 %, 12
[48]	27:63:10	37,600	1.6	8	19.7	-	674	93 %, 6
[48]	45:45:10	49,100	1.5	17	24.8	-	608	67 %, 6
[48]	63:27:10	54,800	1.6	22	25.6	-	570	69 %, 12
D,L-PLGC								
[43]	40:40:20	143,000	1.3	22	7.41	9.19	393	89 %, 7
[43]	30:30:40	124,000	1.3	-6	1.38	3.70	520	77 %, 7
PLGA-PCL-PLGA (D, L-)								
[49]	L:G 50:50	19,200	1.3	22	2.4	26.0	401	63 %, 8
	L:G 75:25	21,000	1.3	29	1.9	19.8	478	50 %, 8
PLLA-PGC								
Block length 2,000 g mol[50]	80:7:13	93,500	1.3	41	34	-	415	60 %, 30
Block length 2,000 g mol[50]	60:13:27	106,000	1.6	40	26	-	363	-
Block length 10,000 g mol[50]	60:13:27	103,000	1.5	47	32.5	-	600	-
PLGT	L:G:T							
L-PLGT								
[53]	20:34:46	33,700	2.1	12	-	3	-	-
[53]	36:37:27	53,900	2.0	31	26	871	>100	-
[53]	52:35:13	48,400	2.0	42	49	1540	8	-
[55]	50:20:30	39,000		30	1.4	-	1450	-
[56]	60:34:6	60,100	2.1	51	44	17.6	300	100 %, 20
[56]	54:34:12	40,000	2.3	44	51	13.3	325	100 %, 17
[51]	73:10:17	39,300	2.4	40	59	1480	-	-
PLGA-PTMC-PLGA (L-)								
[52]	70:10:20	51,100	1.6	44	22.5	294	331	37 %, 24
[51]	74:11:15	42,100	1.7	44	35	1970	-	-

View Article Online
DOI: 10.1039/D0GC01394C

σ = Tensile strength, E = Young's Modulus, ε_b = Elongation at break. All biodegradation studies were carried out at 37 °C in a phosphate buffer solution of pH 7.4

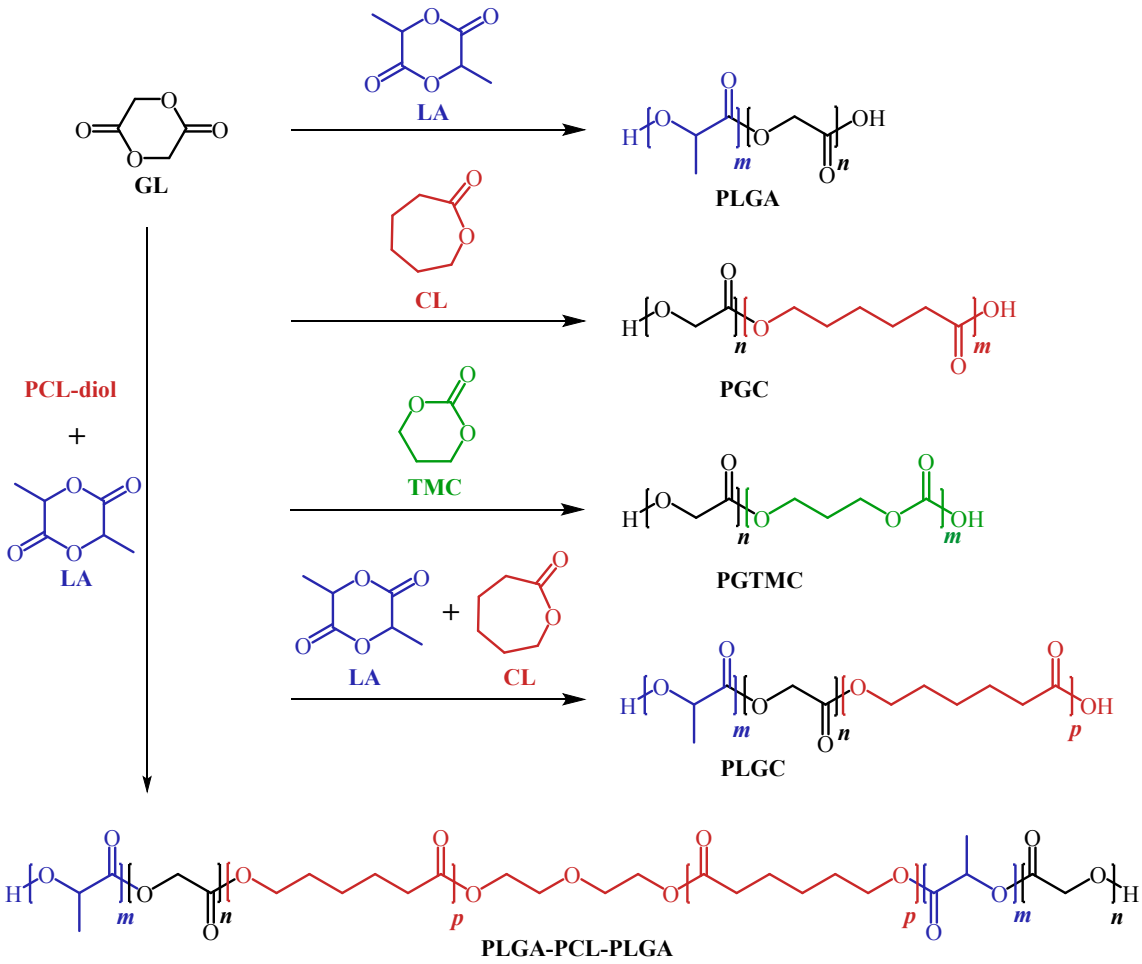

Figure 8: Synthetic routes towards common biodegradable glycolic acid based copolymers. LA = lactide, CL= ε-caprolactone, TMC = trimethylene carbonate, PLGC = (Poly(lactic acid-glycolic acid-co-ε-caprolactone), PGTMC = Poly(glycolic acid-co-trimethylene carbonate), PGC = Poly(glycolic acid-co-ε-caprolactone), PLGA = Poly(lactic acid-co-glycolic acid), PLGA-PCL-PLGA = poly((lactic acid-co-glycolic acid)-block-(ε-caprolactone)-block-(lactic acid-co-glycolic acid))

2.2.6 Other copolymers

There has been a surge of interest in developing new PGA-based materials for a broader spectrum of applications. As such, much literature has been published focusing on PGA-copolymers from a wide variety of monomers, the structures of these co-monomers and the resulting copolymer properties are summarised in Table 6. Various lactones, such β-propiolactone, γ-butyrolactone, and γ-valerolactone have been copolymerized with glycolide.[57-60] However, little data has been published on the properties of these copolymers. Poly(glycolide-co-γ-butyrolactone) (PGB) copolymers were synthesized via the transesterification of PGA with γ-butyrolactone (acting as comonomer and solvent) at 160 °C using $La[N(SiMe_3)_2]_3$ as the catalyst and benzyl alcohol as the initiator. After 2 days, the

copolymer contained 20 mol % γ-butyrolactone and had an M_n of 6,610 g mol^{-1}. Incorporating γ-butyrolactone lowered the T_g (3.7 °C), T_m (107 °C), and T_c (82 °C) whilst increasing the T_d (292 °C), thus improving resistance to thermal degradation. The same PGB copolymer with a similar M_n was also synthesized via ROP, and this material had a lower T_m (241 °C). The differences in thermal stability were attributed to changes in the monomer sequence in the structure. Copolymers formed via transesterification contain B-G-B alternating sequences, which enhance the thermal stability, increasing the T_d. [61]

Mandelic acid is a bio-based alpha hydroxy acid widely used in the pharmaceutical, cosmetics, and food industries. Because it contains a phenyl substituent, researchers have incorporated it into poly(α-hydroxy acid)s, such as PLA to improve thermal properties.[62] Poly(mandelic acid) (PMA) has been considered as a bio-based, bio-degradable alternative to polystyrene.[63] Mandelic acid has been incorporated into PGA to increase its hydrophobicity and T_g, increasing hydrolytic stability, extending its degradation time. Since its cyclic dimer, mandelide, is not commercially available, new cyclic monomers incorporating mandelic acid must be prepared before ROP can be performed.

Nakajima et al. synthesized L-3-phenyl-1,4-dioxane-2,5-dione (PDD), a cyclic dimer of glycolic acid and mandelic acid, this was then ring-opened (150 °C, 3 hours, $Sn(Oct)_2$) to synthesize the random copolymer poly(mandelide-*co*-glycolide) (PMG) (M_n 43,000 g mol^{-1}, M_w 79,000 g mol^{-1}, PDI 1.7, T_g 65.1 °C, no T_m). PDD was also copolymerized with glycolide to produce poly(mandelide-*co*-glycolide / glycolide) with a 50:50 PDD:GL ratio, giving an overall M:G ratio of 20:80, this was of low molecular weight (M_n 8,900 g mol^{-1}), with a T_g of 41°C and T_m of 162 °C, indicating it to be semi-crystalline. PDD was also polymerized with a lactide to produce an amorphous high molecular weight (M_n 40,600 g mol^{-1}) poly(mandelide-co-glycolide-co-lactide) polymer with a T_g of 61 °C that contained 30 % glycolide. [64]

Wang et al. increased the thermal properties of PMG by using regioselective zirconium catalysts to synthesize PMG via the regioselective ROP of PDD. This produced perfectly alternating PMG with a T_g of 91.3 °C (M_n = 45.7 g mol^{-1}).[65]A similar approach of synthesizing new cyclic monomers was used by Amador et al. to copolymerize glycolic acid and 2-methyl-1,3-propanediol (2MD) to produce poly[(glycolic acid)-alt-(2-methyl-1,3-propanediol)] (T_g = -32 °C for M_n 70,000 g mol^{-1}). [66]

Soccio et al. performed the polycondensation ($Zn(OAc)_2.2H_2O$, 190 ~ 230 °C, 25 hours, vacuum) of glycolic acid, and 2-hydroxyisobutyrric acid (HIB) to synthesize poly(glycolic acid-co-hydroxyisobutyric acid) (PGHIB). This introduced two pendant methyl groups into PGA, lowering the T_g and T_m, whilst elevating the temperature of initial decomposition (T_{id}). PGHIB (M_n 20,900 g mol^{-1}) containing 90 mol % glycolic acid showed a T_g of 31°C, a T_m of 180°C and a T_{id} of 331 °C .[67]

Amorphous, hyperbranched PGA copolymers with good solubility in common solvents were obtained by Fischer et al. via the combined ROP/PC (170 °C, 21 hours, vacuum, $Sn(Oct)_2$) of glycolide

and 2,2-bis(hydroxymethyl)butyric acid (BHB). PGBHB copolymers of various compositions were synthesized, these had low M_n (1,100 to 4,000 g mol^{-1}) and lower T_g (24-28°C) than PGA.[67]

Table 6. Properties of PGA copolymers from other monomers

Copolymer	Comonomer Repeat Unit	Structure	GA % / mol %	M_n / g mol^{-1}	Đ	T_g / °C	T_m / °C
Poly(glycolic acid-co-γ -butyrolactone) (**PGB**) [61]	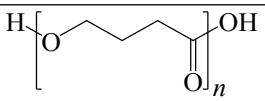 γ-Butyrolactone (**BL**)	Sequence-defined	80	6,610	1.3	4	107
Poly(mandelic acid-*co*-glycolic acid) (**PMG**) [64, 65]	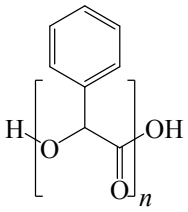 Mandelic acid (**MA**)	Random	50	43,000	1.7	65	-
		Alternating	50	45,700	1.3	91	-
Poly(mandelic acid-co-glycolic acid-co-lactic acid) (**PMLGA**) [64]	MA + LA	Random	30	40,600		61	-
Poly(glycolic acid-co-2-methyl-1,3-propanediol) (**PGMP**) [66]	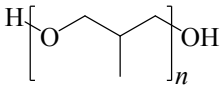 2-Methyl-1,3-propanediol (**2MD**)	Alternating	50	70,000		-32	-
Poly(glycolic acid-co-2-hydroxyisobutyric acid) (**PGHIB**) [67]	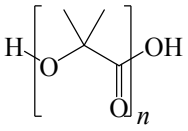 2-Hydroxyisobutyrric acid (**HIB**)	Random	90	20,900		31	180
Poly(glycolic acid-co-bis(hydroxymethyl) butyric acid) (**PGBHB**) [67]	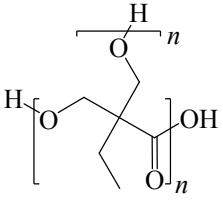 2,2-Bis(hydroxymethyl) butyric acid (**BHB**)	Branched	50	3,980	1.9	24	-

View Article Online
DOI: 10.1039/D0GC01394C

Poly(glycolic acid-co-ethyl 9-(oxiran-2-yl) nonanoate) (**PGEON**) [68]	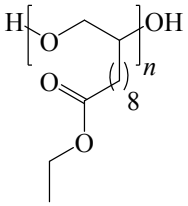 Ethyl 9-(oxiran-2-yl) nonanoate (**EON**)	Random	90	64,100	1.5	8	177
Poly(glycolic acid-co-oxiran-2-ylmethyl palmitate) (**PGOMP**) [68]	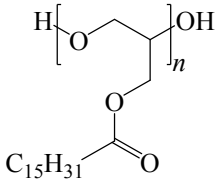 Oxiran-2-ylmethyl palmitate (**OMP**)	Random	95	126,000	1.2	21	178

Using renewable fatty ester epoxide comonomers, Reyhanoglu et al. introduced pendant alkyl groups into PGA, allowing control of thermal properties. These side chains lower polymer crystallinity, lowering the T_g and T_m. The copolymers were synthesized from trioxane, CO, and epoxides using the same conditions used by Goturk et al. (Table 3). They had bimodal molecular weight distributions with high molecular weights (M_n up to 132,000 g mol^{-1}), high glycolic acid contents (90-95 % GA), improved solubility (dissolved in DMF and DMSO) and faster degradation rates than literature values for PGA. Additionally, increasing the epoxide incorporation decreased discoloration. [68]

Various substituted poly(glycolide)s, such as poly(ethylglycolide) and poly(hexylglycolide), have been prepared in which the T_g decreases as the length of the pendant side chain increases. Cyclohexyl-substituted poly(glycolide)s have been synthesized with higher T_g's than PGA.[69] Such polymers could be copolymerized with glycolide to tailor the T_g. Acetylene-functionalized glycolide monomers have also been synthesized to produce PGA-based polymers with pendant acetylene groups for further use in 'click' chemistry.[70]

3. Chemical, thermal, and mechanical properties of PGA

PGA is resistant to commonly used organic solvents but soluble in hexafluoroisopropanol (HFIP) up to a maximum weight of 45,000 g/mol.[7, 20] The melting, crystallization, and glass transition temperature of PGA range between 220~230 °C, 150~180 °C, and 35~40 °C, respectively.[7] Chatani et al. were among the first to determine the crystal structure of PGA as the form of –[$(CH_2)_z$-CO-O-]$_n$– using diffraction patterns of fibers. The data indicated that two molecular chains of PGA pass through the unit cell with an orthorhombic arrangement (Space group P_{cmn}-D_{2h}^{16} with lattice parameters a=5.22

View Article Online
DOI: 10.1039/D0GC01394C

Å, *b*=6.19 Å, and *c*= 7.02 Å) and adopt an all-trans conformation in its crystalline state. 71 The equilibrium melting temperature (T^o_m), the entropy of fusion (ΔS_f) and heat of fusion(ΔH_f) was determined by Nakafuku et al. using the Clapeyron-Clausius equation.[72] T^o_m determined from Hoffman-Weeks plots was found to be 504.6 K while ΔH_f was 183.2 J/g. ΔS_f of PGA was 0.363 J/g/K.

PGA has a high heat distortion temperature (170 °C), which is beneficial for high-temperature applications. It is susceptible to oxidative degradation at elevated temperature, and its thermal degradation temperature is ~ 255 °C, which is close to its melting point.[7, 20] It has weak hydrogen bonding between the hydrogen atoms of CH_2 and oxygen atoms of the ether group in the crystalline structure, which weakens with increasing temperature.[73] Using infrared (IR), Raman spectroscopy, wide-angle X-ray diffraction (WAXD), differential scanning calorimetry (DSC), quantum chemical calculations and natural bonding orbital (NBO) calculations, Sato et al. reported that the intermolecular interactions in PGA chains affects the high-order structure and results in a uniquely high melting point. [74] In a different study, Terahertz (THz) spectroscopy, a two-dimensional correlation (2D-COS) of WAXD profiles along with IR spectroscopy was performed on isothermal crystallization of PGA to probe the higher-order conformation, crystalline structure, and intermolecular interactions. At the same time, the development of crystals occurred in PGA. The vibrational motion detected in the THz region is predominantly due to the inter- and intra-molecular vibrations. At lower vibrational frequency, intermolecular vibrations are dominant, while intramolecular vibrations seen for absorption bands at high frequency. There are two signature bands for PGA, both being vertical vibrations concerning the c-axis. The temporal difference in these two bands during isothermal crystallization can be thought of as the difference in the formation between short-range and long-range order.[73] The band at 65 cm^{-1} is due to the out of plane bending of the C=O group, which is sensitive to changes in the inter-chain distance of crystalline PGA, and this band exhibits a redshift when PGA is subjected to heat due to thermal expansion in its crystalline lattice.[73] The group at 192 cm^{-1} is due to the twist/rocking of CH_2 along with the deformation of the O-CH_2 bond and is independent of the temperature shift. The CH_2 rocking and O-CH_2 deformation are ascribed to twisting of the local structure of PGA chains. For 2D-COS analysis of WAXD profiles, crystallization was carried out from 6 s to 366 s at 185 °C, and it was observed that the intensities in the diffraction peaks (110) and (020) observed at 2θ 14.2° and 18.1° increased with time. Further, along the (110) direction, C-H···O (ether) hydrogen bonding exists. It also appears in PGA microcrystals in the early stages of crystallization.[73] A comparison of the crystallinity, melting temperature (T_m), enthalpy of fusion (ΔH_m), and long period (L) of common biodegradable polyesters poly (L-lactide) (PLLA) and poly (ε-caprolactone) (PCL) with PGA was done by Baez et al. using DSC and small-angle X-ray scattering (SAXS). [75] They observed that with a similar number of average molecular weight (M_n), T_m was dominated by the polarity of the structural unit of the ester and followed the trend PGA > PLLA > PCL wherein alkyl end groups had a negligible effect on the same. ΔH_m followed the pattern PGA > PCL > PLLA, and the crystallinity for relatively polar PGA was

slightly affected by the alkyl ends attributed to steric hindrance effects. In contrast, for relatively non-polar PLLA and PCL, the impact of the alkyl end group on crystallinity was not significant. In this context, the crystallinity and L followed the trend PCL>PLLA>PGA.[75]

The arrangement of crystalline domains, the skeletal conformation of molecular chains, and the intramolecular interactions play a key role in the manifestation of elastic modulus in PGA. To prove this, Lee et al. measured the crystal modulus (elastic modulus of the crystalline domains) of PGA using X-ray diffraction in the longitudinal (E_l) and transverse (E_t) directions to the chain axis.[76] Crystal modulus determination involves the use of a cryogenic setup, cryostat cell, stretching device, and a load cell. This is mounted on an X-ray goniometer. E_l, which was measured along (006), was 104 GPa at room temperature, relatively low resembling that of poly (ethylene terephthalate) having a value of 106 GPa. This value was lower that of polyethylene, which is around 235 GPa, which suggests that the PGA skeleton was contracted and not in fully extended form. E_t measured along (110) was 7 GPa, resembling the modulus of poly(vinyl alcohol) due to intermolecular hydrogen bonding. At 200 K, there were abrupt changes in both E_l and chain contraction of PGA. Along with this, an increase in tan δ was observed, indicating that segmental motion in the crystalline domains of PGA was also activated at this temperature. Furthermore, according to this study, low E_l and high E_t values contributed to the unusually high melting point of PGA among all the reported polyesters.[76]

The stereoregularity in PGA also makes it more stiff and rigid in comparison to other biodegradable polymers. Table 7 compares the thermo-mechanical properties of PGA with other commercial biodegradable polymers. The high mechanical and thermal properties of PGA are even competitive to common and engineering plastics. As shown in the materials properties chart in Figure 9 (a), the maximum service temperature of PGA is outstanding, higher than PET and PA6, even close to PEEK. It is much higher than other biopolymers such as PCL, PHA, PLA, and PLGA. This indicates that PGA could be developed for high-temperature applications, such as biodegradable packaging materials for hot food, clothing, or electronics. Figure 9 (b) compares the mechanical properties of PGA with other commercial polymers. PGA has the strongest mechanical strength but lowers fracture toughness similar to PHA, which is much lower than PLA, PLGA, and PET. This is mainly due to its high crystalline structure. Further modifications of PGA are needed to improve its flexibility and toughness, such as by copolymerization or blending with other flexible polymers. This will be discussed in section *5.5.2*.

Figure 9 (c) shows the permeability properties (oxygen and water vapor) for some commercial polymers along with PGA. The reported normalized values for the oxygen permeability, CO_2 permeability and moisture permeability of PGA are 0.014 $cm^3 \cdot mm/m^2 \cdot d \cdot atm$, 0.052 $cm^3 \cdot mm/m^2 \cdot day \cdot atm$, and 0.2 $g \cdot mm/m^2 \cdot day$ respectively.[77] Although PGA and PLA belong to the same family of biodegradable polyesters, PLA exhibits relatively poor oxygen and moisture barrier properties with oxygen permeability of ~540 $cm^3 \cdot mm/m^2 \cdot d \cdot atm$, and moisture permeability of ~1.96 $g \cdot mm/m^2 \cdot d$.[78] Interestingly, the barrier properties of unmodified PGA is much superior to cellulose nanocrystals

(CNCs) loaded PLLA, low concentration (0.05 wt%) graphene oxide loaded Pullulan as well as 2 wt % loaded polystyrene graphene oxide composite.[79-81] This plausibly indicates that PGA has the capabilities in manifesting superior barrier performance if it is combined with 2D layered materials like graphene oxide etc. Further, high gas-barrier properties and high thermal processing temperature of PGA make it suitable to laminate with PET by co-extrusion or substitute PET films for food packaging applications, which will highly expand the applications of biodegradable polymers.

Table 7. Thermo-mechanical properties of some commercial biodegradable polymers.

Polymer	T_g (°C)	T_m (°C)	Tensile strength (MPa)	Young's Modulus (GPa)	Elongation at break (%)
Poly (glycolic acid) (PGA)[7] 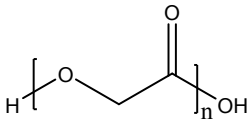	35~40	220~230	115	7	1~3
Poly (hydroxybutyrate) (PHB) [82, 83] 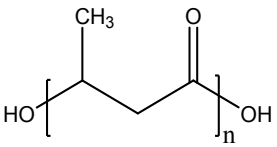	-1	160 to 170	40	1.7-3.5	3~6
Poly (butylene succinate) (PBS) [84, 85] 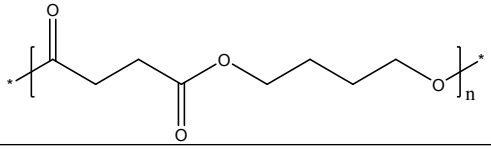	-32	110~120	32.1	0.33	321
Poly (lactic acid) (PLA)[82, 86] 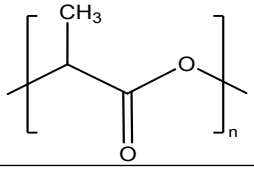	50 to 60	140~180	28-50	1.2~2.7	5~9
Poly(trimethylene carbonate) (PTMC)[87, 88] 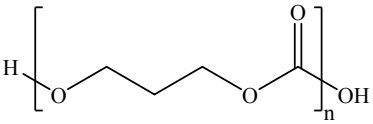	-19 to -27	-	1.8-2.4 (stress at yield)	0.005-0.006	610~670
Poly (ε-caprolactone) (PCL)[82] 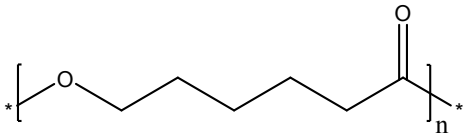	-60	60	16	0.4	120~800
Poly (3-hydroxybutyrate-co-3-hydroxyvalerate) (PHBV) [82, 89] 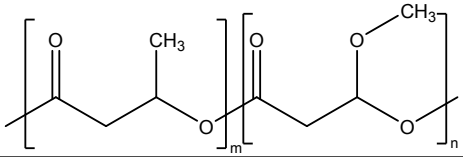	1.4 to 2.8	170	30-38	0.7-2.9	20

Poly (butylene adipate-co-terephthalate) (PBAT) [90, 91] 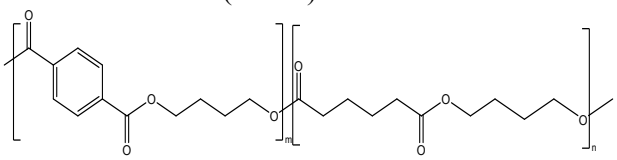	-30	110 ~ 120	11-20	0.04-0.08	500~800
Poly [(butylene succinate) -co- (butylene adipate)] (PBSA) [92] 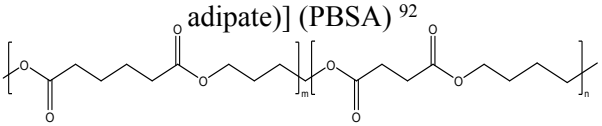	-30 to -40	89 ~ 97	15.6	0.16	408
Poly (L-lactide-co-glycolide) (PLGA)[14, 41] 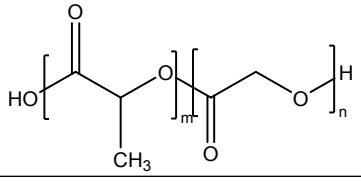	40-60	100-200	40-90	2-4	<10
Poly (lactide-co-caprolactone) (PLCL)[93] 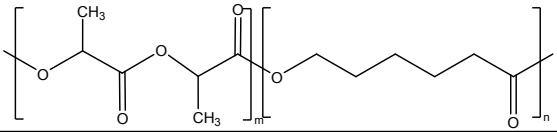	16.4 to 57.3	136 ~ 174	17.2-26.6	0.01-1.34	314~486
Poly (glycolide-co-caprolactone) (PGC) [93, 94] 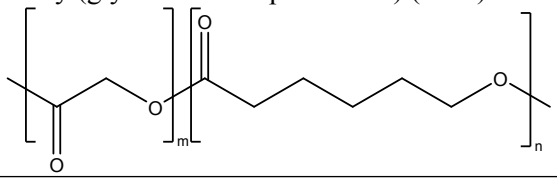	-60 to -12	-	0.6	0.4-1.7	>250 %
Poly (lactide-co-glycolide-co-caprolactone) (PLGC)[45, 48, 93] 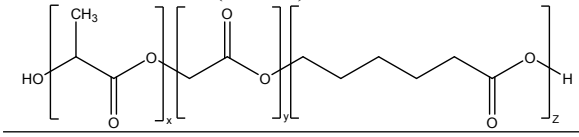	-57.8 to 22	-	0.01-31.5	0.02	500~1356

Note: The stated values of mechanical properties for these polymers are critically dependent on the molecular weight, % crystallinity, and the conditions (like cross-head speed) used during mechanical testing.

View Article Online
DOI: 10.1039/D0GC01394C

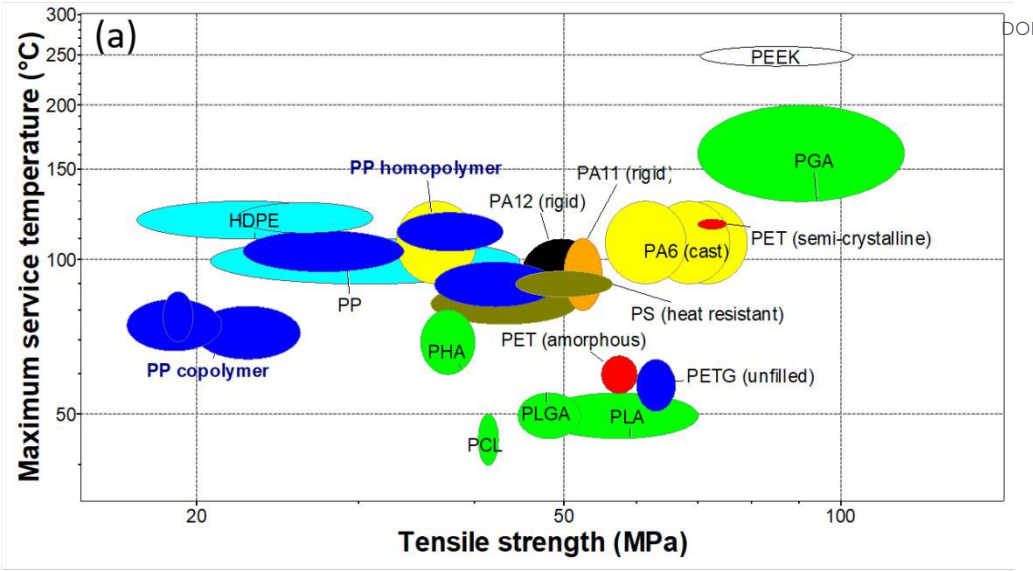

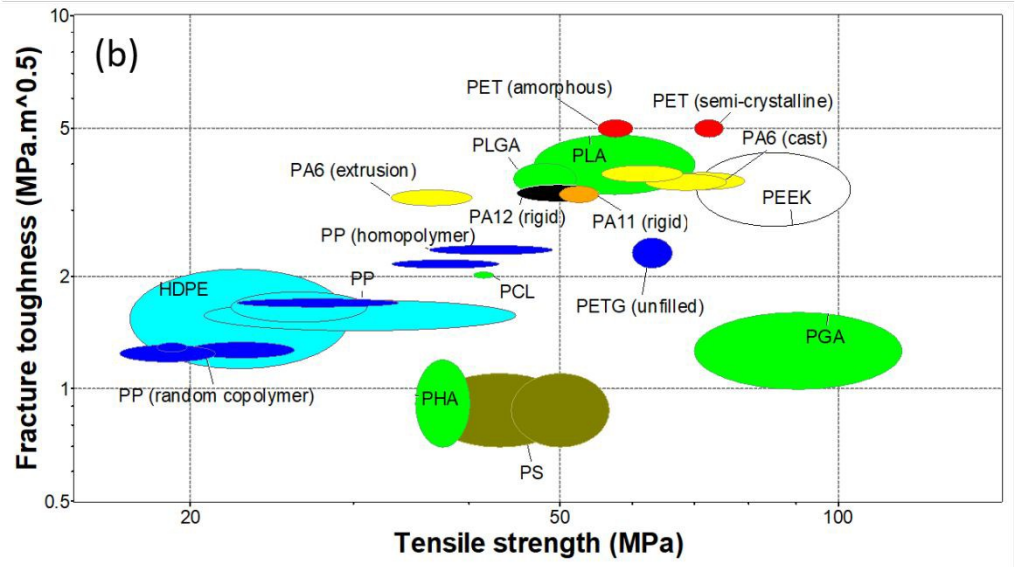

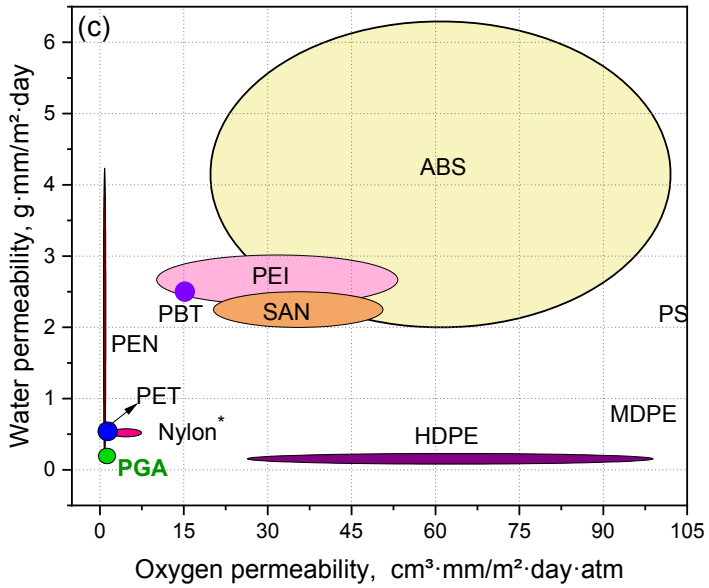

Figure 9: Material properties chart created using CES Edupack 2019, comparing the properties of PGA with common commercial polymers: (a) Maximum service temperature vs. tensile strength (b) Fracture toughness vs. Tensile strength. (c) Water vapor permeability vs. oxygen permeability of some common commercial polymers. (*The reported values are normalized values for Nylon, PBT and PET for DuPont Selar Amorphous Nylon, BASF AG Ultradur PBT, and PET Mylar 800 taken from ref.[77] while the rest normalized values are taken from ref.[95])

4. Biodegradation characteristics of PGA and its blends

In biodegradable polymers, the degradation process can be initiated by non-biological processes like hydrolysis and erosion or by biological means like enzymatic action or by microorganisms such as bacteria, yeast, and fungi. These processes can work in tandem to accelerate the degradation in these polymers.[96] In non-biological processes, chemical scission, along with physical erosion, is primarily responsible for degradation.[97] For polyesters like PGA, the chain scission generally starts from the hydrolytically labile ester linkages.[98] The amorphous domains are more prone to the diffusion of water molecules; hence hydrolytic degradation occurs first in the amorphous regions of the polymer leading to chain scission. In the later stage, the crystalline parts undergo hydrolytic degradation.[99] It is important to note that the extent of hydrolysis is critically dependent on the relative hydrophilicity of the polyesters involved. Among the known biodegradable polyesters, PGA is reported to have relatively high hydrophilicity, followed by PLA. PCL is relatively less hydrophilic than PGA and PLA. Hence, the rate of hydrolytic degradation in PGA is quite intensive to that in PLA and PCL.

Physical erosion accompanies hydrolysis aiding in degradation. Physical erosion can be either (a) bulk erosion or (b) surface erosion. While bulk erosion is associated with the entailment in mass loss throughout the material while the surface erosion is limited only to the exposed specific surfaces and proceeds via an erosion front.[100] In the case of biodegradable aliphatic polyesters like PGA, bulk erosion is prominent, leading to specimen fragility and compromises the mechanical and functional capabilities of the materials.[101]

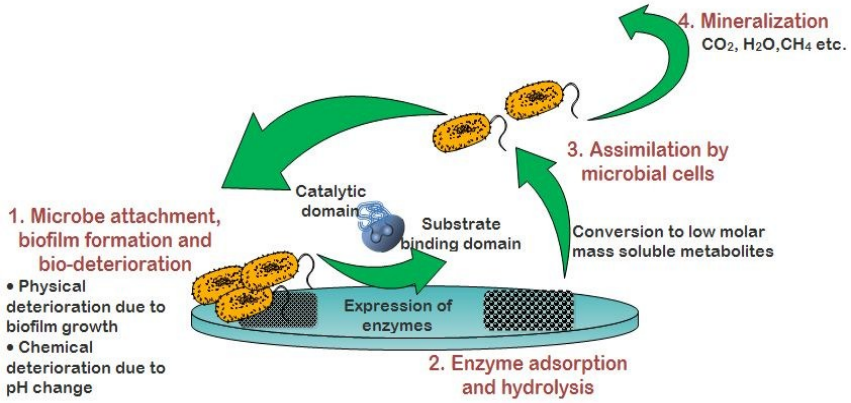

Figure 10: Biological degradation of polymer substrate by bacteria. For enzymatic degradation, just step 2 is observed.

Biological degradation can occur via microbes or enzymatic action. In general, the degradation progresses in four steps, as illustrated in Figure 10. The first step is bio-deterioration, wherein superficial degradation by decomposer microorganisms leads to chemical and physical deterioration of the plastics. The physical deterioration is caused by the formation of microbial biofilms, which penetrates surface topological pores or micro-cracks, leading to provocation and deterioration in physical properties.[102] Chemical deterioration follows the physical deterioration and is caused by a drastic change in pH due to the release of acidic substances by the biofilms, like nitrous acid, by organisms like *Nitrosomonas* spp., sulfuric acid by *Thiobacillus* spp. and nitric acid by organisms like *Nitrobacter* spp..[103] Apart from this, organic acids like citric, gluconic, fumaric, oxalic, glutaric, glyoxylic, and oxaloacetic acid can also be observed in these processes.[103] Bio-deterioration is followed by bio-fragmentation, where the catalytic actions by specific enzymes cause depolymerization and/or chain cleavage, leading to the formation of oligomers. Extracellular enzymes or exoenzymes like oxygenase first incorporate one/two oxygen atoms in the polymer chain aiding in the creation of alcohol or peroxyl functionality. This is followed by exoenzymes like lipases, esterase, and endopeptidase, depending on the type of polymer involved. For esters like PHB, PHBV, PCL, and PGA, pseudomonas is the predominant genera to cause bio-fragmentation. [103] The last two processes are assimilation and mineralization.

In the case of PGA, the monomeric unit glycolic acid is a natural metabolite that is directly taken up by the microbial cells. Mineralization is the complete degradation of primary and/or secondary metabolites leading to by-products like minerals, water, and biomass. It is critical to note that biodegradation mediated via enzymes mimics the synthetic chemistry wherein the enzymes act as catalysts that induce an increase in reaction rate for degradation.[96] The active sites in the enzymes interact with the substrate and lead the chemical reaction. For the maximized activity, some enzymes may require co-factors like metal ions or co-enzymes and vitamins.[96] Hence, the micro and macro environment surrounding the polymer substrate also determines the rate of biodegradation of these polymers.

Shawe et al. studied the rate of degradation of PGA using in-vitro degradation, DSC, and gel permeation chromatography (GPC). It was observed that during significant degradation of PGA, the degree of crystallinity increased from 31 % to 56 % in 24 days, which validates the mechanism of hydrolytic degradation wherein the amorphous regions are labile to hydrolysis first. A significant drop of molecular weight from 30,000 to 5000 $g \cdot mol^{-1}$ was observed within the 3rd day of degradation and stabilized at around 2500, inferring that the minimum molecular weight to facilitate diffusion was around 2500 $g \cdot mol^{-1}$. [104] Hu et al. studied the growth and non-biological degradation of PGA and PCL based polymer brushes. Ring-opening polymerization was performed with both the sets of monomers with tin octanoate as the catalyst, and it was observed that the PCL brushes grew thicker at elevated temperatures. In contrast, PGA based brushes were most abundant at room temperature. Unlike bulk polyester, which can degrade in acid as well as basic mediums, the confined surface polyester brushes

only degraded in basic and neutral conditions. The degradation mechanism of these brushes was investigated using a blocking test, and it was observed that the terminal hydroxy groups were primarily responsible for initiating the degradation of these brushes via the backbiting mechanism. [105]

Vieira et al. analyzed the degradation rate of hybrid and single fibers of PLA-PCL, PGA-PCL, poly dioxane (PDO), and PGA in water, sodium chloride solution, and phosphate buffer saline.[106] Among all the samples, hydrolytic degradation was fastest in PGA-PCL and followed by PGA, PDO. PLA-PCL was least in terms of degradation. The mechanism of hydrolysis was modeled using first-order kinetics according to the Michaelis-Menten scheme. Similar to the report by Hu et al. [105], the degradation of PGA-PCL and PGA was more considerable in basic conditions (PBS) followed by neutral conditions (in water).

Cruz et al. investigated the hydrolytic degradation of electrospun PGA thin films incorporated with titanium oxide (TiO_2) nanoparticles.[107] Incorporation of these nanoparticles accelerated the hydrolytic degradation in phosphate buffer (with pH 7) for a study period of 8 weeks because TiO_2 is hygroscopic. Further, its anatase phase can absorb water more than the rutile phase. It was observed from this work that the incorporation of these nanoparticles enhanced the thermal stability of the system and slow thermal degradation. In a study by Rouhollahi, the biodegradability and bactericidal properties of hybrid sutures of PGA-PLGA nanofibers incorporated with silver were studied. Incorporation of 3 wt. % of silver nanoparticles manifested considerable response to both *E.coli* and *S.aureus*.[108] The degradation studies were carried out in phosphate buffer of pH 7.4 for two weeks, and it was observed that the mechanical strength and elongation at break of the fibers was decreased by 12 % and 93 % respectively within three days. The samples became fragile after seven days of incubation.

The enzymatic degradation of PCL and PGA blend based electrospun fiber was assessed using pseudomonas lipase by Spearman et al.[109]. The fibers were impregnated in double-stranded deoxyribonucleic acid wrapped singe-walled carbon nanotubes and encapsulated in a PCL matrix. Pseudomonas lipase was then used to catalyze the degradation. The composites were able to exhibit considerable degradation within four weeks.

PGA and poly (methylene oxide) (PMO) based inflow control devices (ICDs) were used in conditions mimicking Brazilian offshore oil wells by Pereira et al.[110] ICDs in these wells can provide friction loss by channeling fluids (such as in acid treatments) through a designed set of holes. The imposed friction loss alters the natural formation flow profile during oil injection or production. In their study, PMO and PGA samples were subjected to chemicals, like hydrochloric acid (HCl) and sodium chloride (NaCl) solutions and xylene as channeling fluids. From the chromatographic analysis, it was inferred that PGA and PMO were unaffected with xylene exposure. Further, the hydrolytic degradation of PGA was extensive in brine with temperatures above 75 ^{o}C, and when compared to PMO, PGA was more susceptible to acid hydrolysis.

View Article Online
DOI: 10.1039/D0GC01394C

5. Applications

The potential applications of PGA and its derivatives in critical areas of drug delivery and tissue engineering, degradable packaging, functional coating, and patches now discussed.

5.1 PGA based composites in tissue engineering and drug delivery

Owing to its ease of degradation by hydrolysis followed by bulk erosion and compatibility to resorb into the system through metabolic pathways (the degradation byproduct glycolic acid is a natural metabolite), PGA has been one of the accessible, sustainable materials in clinical applications.[99] The presence of functional moieties in the structural unit allows tailoring the degradation rates to suit different applications. Table 8 shows the recent advances in tissue engineering and drug delivery involving PGA as one of the critical materials.

Table 8. Critical applications of PGA and its composites in drug delivery and tissue engineering

Materials involved	Application	Key features
PGA and PCL[111]	Esophagus prosthesis	• Tubular knitting of PGA braided yarns and PCL nanofibers. • Knitted tubular fabrics have mechanical properties similar to real esophageal tissue
Hyaluronic acid and PGA[112]	Cartilage formation	• 1 % hyaluronic acid coating on PGA scaffolds exhibited less inflammation in-vivo. • Coated PGA could engineer cartilages with high collagen and glycosaminoglycan content in-vitro.
Collagen and PGA[113]	Bone defect healing	• Collagen sponge with PGA for calvaria bone defect regeneration in rabbits.
PCL, Tea polyphenol, PLA and PGA[114]	Drug release	• Sutures with different degradation rates to carry drug of tea polyphenol. • Higher PGA content leads to faster drug release in sutures.
PLA and PGA[115]	Acupoint catgut embedding therapy application	• Monofilament melt-spinning of PLA and PGA. • All samples were not toxic, and PLA degraded slower as compared to PGA.
PGA and fibrin[116]	Partial glossectomy	• Covering open wounds using the PGA sheet aided with fibrin glue spray after partial glossectomy. • Clinical evaluation of 44 patients showed rapid relief from postoperative pain and scar contracture.
Poly (ethylene terephthalate) (PET) and PGA[117]	Drug-eluting vascular graft	• Co-electrospinning of PET and PGA fibers. • A method for sustained local drug delivery having quick release within a prosthetic artery bypass graft.
PLA and PGA[118]	Treatment of noncontained human periodontal infrabony defects	• 16 one/two walled intraosseous errors were randomly divided for decalcified freeze-dried bone allograft, alone and in combination with PGA and PLA membranes. • Non-significant clinical and radiological differences in regenerative outcomes in the treatment of defects.

PCL and PGA[119]	Articular cartilage tissue engineering	• Effect on mechanical, morphological, and physical properties of PCL/PGA scaffolds with cryo-milling. • 12 min, 30 min, and one h milled scaffold mimic human articular cartilage in terms of its compressive modulus and 12 min cryo-milled sample optimum for chondrocyte growth.
Poly (ethylene oxide), PCL, and PGA[120]	Tissue engineering	• Scaffolds prepared by combining cryo-milling, compression molding, and polymer leaching. • Scaffolds exhibited co-continuous morphologies with the porosity of ~50 %.
Silk fibroin and PGA[121]	Bone regeneration	• Silk fibroin membranes and PGA based scaffolds prepared by combining electrospinning and hot-melt additive manufacturing. • Within eight weeks, in-vivo rabbit calvarial defect regeneration was achieved.
PGA and collagen[122]	Gait recovery in a rat sciatic nerve	• Regeneration of myelinated fibers was observed in 87.5 % of rats.
PCL and PGA[123]	Bactericide drug delivery	• PCL/PGA based continuous fibers were electrospun, and curcumin and polyhexamethylene biguanide as hydrophobic and hydrophilic bactericide compounds were loaded. • All samples showed a bactericidal effect in cell culture and agar media.
PGA, collagen, and bioglass[124]	Potential for nerve generation	• Electrospinning of PGA, collagen, and nanobioglass was performed. • Scaffolds are more suitable for cell adhesion and proliferation in comparison to PGA and PGA/collagen.
PGA[125]	Promising islet cell scaffold	• PGA modified by plasma followed by polylysine coating and combined plasma and polylysine coating. • Plasma, along with polylysine coating, enhances adhesion and biocompatibility.
Poly-4-hydroxybutyrate (P4HB) and PGA[126]	Potential autologous therapy of intracardiac wall defects	• Non-woven PGA meshes coated with 1.75 % P4HB were seeded with human umbilical cord-derived cells and exposed to static and dynamic conditioning. • Dynamic conditioned specimens showed higher collagen that static ones.
PGA[127]	General biomedical application	• Immobilization of biotin on PGA sutures by NHS activation chemistry.
PGA[128]	Myringoplasty	• PGA sheets used as reinforcement along with tympanic membrane perforations. • After 4 to 5 weeks of post-operation complete epithelialization was observed.
PGA and fibrin[129]	Pneumothorax surgery	• Poly (glycolic acid) membrane adhered to a surface of a bulla with fibrin glue. • This was effective in preventing the recurrence of pneumothorax.
PGA and collagen[130]	Proliferation and differentiation of rat bone marrow stromal cells	• PGA, collagen, and PGA-collagen based mixture sponge was generated with and with UV irradiation. • PGA-collagen with and without UV irradiation were useful in manifesting bone regeneration.

PGA[131]	Tissue engineering	• Hydrochloric acid pre-treatment was done on PGA scaffolds, and biocompatibility was assessed in-vitro and in-vivo using a rat model. • Improvised biocompatibility of PGA with acid pre-treatment.
PGA and sodium alginate[132]	Surgical application	• Reinforced structure derived from PGA mesh with sodium alginate-based foamy matrix. • This foam strongly inhibited the PGA induced adhesion and provided secure handling in surgery.

5.2 PGA and its composites in structural and functional applications

Apart from the applicability to personalized drug delivery and tissue engineering applications, the high mechanical properties and gas-barrier performance of PGA make it very promising for engineering applications such as coatings, membranes, thermal management, sensing, packaging, and structural applications.

5.2.1 PGA in coatings, sensors, actuators and thermal management

PGA provides a sturdy template for a modified fungicide that can serve in antifungal coated materials. Boehm et al. fabricated microneedle arrays of PGA with an elastic modulus of 9.9 ± 0.3 GPa, hardness 588.2 ± 33.8 MPa and sharp tip radius of 25 ± 3 μm by combining injection molding and draw lithography. Voriconazole mixed with poly(methyl vinyl ether-co-maleic anhydride) was deposited onto this via inkjet printing, and these microneedles showed good antifungal activity against *C. albicans*.[133] In a different study by the same group, they used the same approach with a different drug, itraconazole and, demonstrated the release in porcine skin. These microneedle arrays were also able to demonstrate a zone of inhibition with *C. albicans*.[134]

A self-reinforced polyglycolide membrane with high strength retention was reported by Ashammakhi et al. [135] The layer consisted of braided and knitted PGA fibers, which were glued with PGA on one side as support. The material lost its integrity when subcutaneously implanted in rats in around four weeks, while in immersed conditions in water, the mechanical properties were not measurable only after five weeks.[135] In a different study by the same group, these membranes helped achieve osteogenesis in rats.[136]

PGA has also shown effective capabilities in heat transfer for medical device which employs ferromagnetic heating. In this system, localized heating to intravascular treatment sites can be achieved by positioning the catheters in close proximity and applying an alternative magnetic field (200 kHz to 10 MHz). John Chen patented a device which contains ferromagnetic materials in inner and/or outer layers of the device while the polymer used to encapsulate this can be made of PGA as well as its copolymer derivatives.[137]

In a simulation study by Tariq et al., the capabilities of poly (dimethylsiloxane), poly (methyl methacrylate), and PGA were investigated for actuators in a piezoelectric micro-pump. Using finite element analysis and simulation techniques, these materials were subjected to different voltages ranging

from 50 to 150 V and variable frequencies ranging from 50 Hz to 150 Hz. It was observed that a maximum deflection of 67 μm at 150 V was observed for PGA, and it was the best among the materials tested for piezoelectric micro-pump applications.[138]

David J. Vachon patented a technique to make a biosensor for subcutaneous implantation with an anti-inflammation response, reduced biofouling, and high sensor performance. The fiber material used for this purpose can be a polyester suture from PGA.[139]

5.2.2 PGA in packaging applications

The use of PGA as a potential biodegradable packaging material was first realized in 2005 when Peter M. Bonutti patented a technique to enclose perishable foods, medicines, medical implants, or goods with limited shelf-life using PGA as the film material. The packaging film was made from two layers of PGA with a reactive chemical layer interposed between two. When one layer degrades, the synthetic layer is exposed to air and causes the color change in the remnant layer, an indication of the expiry of the shelf-life of the package.[140]

In 2011, Hokari et al. patented a technique to derive a paper-like multilayer laminate of PGA with a molecular weight ranging from 30,000 to 6,00,000 g/mol for potential application in disposable cups for coffee, soup, noodles and other beverages or materials for trays used in pizza, dishes and food for microwave ovens. In one example, it involved four single-layered pressed sheets of PGA with a strength promoter like saccharides (D-glucose and maltose), thickened polysaccharides (xanthan gum, guar gum, etc.), and celluloses (pulp, sugar alcohol, and ester) subjected to heat-pressure bonding and forming at 150 ^{o}C. The laminate had an oxygen permeability constant of 8 cc/m/day/atm at 23 °C and relative humidity 80%. The water vapor permeability was 25 g/m/day at 40 ^{o}C with 90 % relative humidity.[141]

In 2013, Solomon Bekele patented a technique to produce PGA based pouches with gas barrier and odor properties for use in medical packaging. This was achieved via a multilayer approach in which at least one layer comprised of a blend of noise-dampening polymer (like ethylene-vinyl acetate grafted with maleic anhydride) and 40-80 % of PGA resin. The oxygen transmission rate was less than 60 cc/m^2.day.atm at 22.7 ^{o}C and 100 % relative humidity. The storage modulus was about 0.25 GPa at 40 ^{o}C.[142]

In 2015, Vartiainen et al. reported a technique to fabricate multilayer barrier film with lower oxygen transmission rates and high heat seal strength. In their work, one of the samples involved two layers of bio-derived polyethylene (Bio-HDPE one layer and Bio-LDPE one layer) adhered to poly (glycolic acid) interlayer using Lotader AX 8900 (a terpolymer of ethylene, acrylic acid, and glycidyl methacrylate) extrusion coating. Lowest oxygen transmission rates were observed in 50 % and 80 % relative humidity samples for the multilayered film with high heat strength of 690 ± 160 N/m.[143]

Besides the above direct applications, copolymers of PGA have currently made a major impact on antimicrobial packaging, preservative food packaging, barrier films, and composite design. Table 9

shows the recent advances of polyglycolide copolymers in these applications. These copolymers address the key limitations of PGA, like its low extension at the break and quick degradation characteristics by tailoring the structural properties for the desired application.

Table 9. Recent advances of glycolide co-polymers in antimicrobial packaging, preservative food packaging, barrier films, and composites.

Co-polymer and materials used	Application	Key features
Polylactide-co-poly(glycolide-co-caprolactone) multiblock (PLAGC) co-polymer[50]	Biodegradable shape memory films	• PLAGC was synthesized by the coupling reaction of macrodiols (PLLA-diol) and poly(glycolide-co-caprolactone) (PGC-diol) in the presence of 1,6-hexanediisocyanate as a coupling agent. • PLAGC had fast degradation and a more than 90 % strain recovery rate.
Inconnel coated on PLGA crosslinked with diphenylmethane diisocyanate[144]	Biomimetic sensor	• Can be used for inexpensive real-time detection of microorganism spoilage on the product. • After microorganism attaches and grows, the lytic enzyme release from them changes the color of the packaging material, indicating spoilage.
AgNPs in PLGA[145]	Antibacterial nanocomposite films	• Oxygen plasma treatment PLGA/Ag nanocomposites. • Composites with surface treatment had a better reduction of bacteria as compared to unmodified nanocomposites.
Eugenol and trans-cinnamaldehyde in PLGA[146]	Antibacterial nanoencapsulation in smart food packaging	• High loading efficiency of eugenol and trans-cinnamaldehyde of 98 % and 92 %. • Inhibition of *Salmonella* spp. and *Listeria* spp.
Anethole and Carvone in PLGA[147]	Antibacterial essential oil loaded nanoparticles in food application	• Nanoprecipitation method was used with a drug loading of 14.73 % for anethole and 12.32 % for carvone, respectively. • Was able to inhibit *S. typhi*, *S. aureus* and *E. coli*.
Nisin in PLGA[148]	Antibacterial films	• PLGA cast film was loaded with a Nisin solution. • 5 h loading time gave maximum bacterial inhibition to *L. sakei*.
Lysozymes in PLGA[149]	Antibacterial extrudates	• Hot-melt extrusion performed using a syringe-die device. • Inhibition of *Micrococcus lysodeikticus*.
Cinnamon bark extract in PLGA[150]	Antibacterial nanoencapsulation in smart food packaging	• Maximum loading efficiency of 47.6 %. • Effectively inhibited *S. enterica, S. typhi,* and *Listeria monocytogenes*.

PLGA, poly(L-lactide-co-ε-caprolactone) (PLCL) and tricalcium-phosphate-loaded (TCP) composites[151]	Additive manufactured scaffolds	• 20 % and 40 % TCP loaded scaffolds were engineered using modified fused deposition modeling. • The lay-down pattern was 0^o and 90^o.
PLA and PLGA[152]	Biodegradable films	• Polymer blending was done with PLA and PLGA using melt compounding. • Improvement in thermophilic anaerobic degradation was observed in a copolymer blend.
PLLA and PLGA[153, 154]	Multilayered polymer particles in food preservation	• The emulsion solvent evaporation technique was used to fabricate multilayered PLLA and PLGA loaded with benzoic acid. • Excellent activity of these particles for antibacterial and antioxidant activities.
Poly (butylene furan dicarboxylate-co-glycolate) (PBFGA) and Poly (butylene furan dicarboxylate)-b-poly (glycolic acid) (PBF-b-GA)[155]	Sustainable gas barrier packaging material	• Co-polymers synthesized by melt oligomer polycondensation and melt bulk transesterification. • Superior mechanical, thermal, degradation, and CO_2 and O barrier properties observed for PBFGAs.
4-Hexylresorcinol and PLGA[156]	Antibacterial films in packaging	• 4-Hexylresorcinol loaded in PLGA films using solvent casting. • Films were effective in inhibiting Gram-negative, and Gram-positive bacteria, yeasts, and filamentous fungi.
PLGA[157]	Water vapor barrier films	• Sodium hydride based green polymerization of PLGA. • Reduced water vapor permeability as compared to homopolymer PLA and PGA.
PLGA[158]	Non-woven fabrics in forensic engineering	• Tin-free PLGA non-woven fabrics designed and degradation studies were evaluated under abiotic conditions.
Poly DL-lactide-co-ε-caprolactone) (PLCA) and PLGA[44]	Flexible elastomeric blends applications	• PLCA and PLGA were synthesized, and their blends were evaluated for thermomechanical properties. • With an increase in PLGA content, the tensile strength increased while elongation at break decreased.

Besides the use of copolymerization approaches for target applications, functional polymer blends and nanocomposites of PGA can manifest desired results via the incorporation of suitable polymer counterparts and nanofillers. As discussed previously, among PLLA, PCL, and PGA, PGA has the highest polarity, and its specific interactions with other polar and non-polar polymers will dominate the considerations for functional polymer blends. Madkour et al. employed molecular dynamics

View Article Online
DOI: 10.1039/D0GC01394C

techniques to evaluate the enthalpy of mixing, the entropy of mixing, the loss in entropy due to the deformation of the polymeric chains upon mixing and the total free energy change for a series of five polar and non-polar PGA polymer blends namely, PGA/poly (3-hydroxybutyric acid) (PHBA), PGA/PHVA, PGA/PCL, PGA/ polyglutamic acid (PGlu), and PGA/ isotactic polypropylene (iPP). It was observed that PGA/iPP blends had the highest positive interaction parameter, and the trend (in the decreasing order of interaction parameter) was PGA/iPP> PGA/PHVA> PGA/PHBA> PGA/PCL> PGA/PGlu indicative that PGA was highly immiscible with non-polar iPP. Further, negative enthalpy of mixing was observed in PGA/PHVA and PGA/PHBA blends, which suggested specific interactions between PGA and PHVA, PGA, and PHBA, respectively. They also concluded that the PGA/PHBA blend was highly miscible at all volume fractions of PGA due to the large attractive binary interactions between PGA and PHBA. Similarly, the PGA/PCL blend showed high miscibility at high PGA concentrations, and PGA–PGlu blend showed high miscibility at low PGA concentrations, mainly due to the formation of hydrogen bonding. In all these cases, the enthalpy of mixing was high enough to overcome any loss in entropy due to the deformation in the polymeric chains. PGA/PHVA showed moderate miscibility at all volume fractions of PGA while PGA/PCL was miscible for all volume fractions of PGA.[159]

Essentially from this study, it is clear that PGA is highly immiscible with non-polar polymers, e.g., PP and other olefin derivatives, and relatively miscible with polar polymers. However, the poor miscibility of PGA and PP can be improved by adding a suitable compatibilizer to the blends. Yang et al. used maleated ethylene octene copolymer and attapulgite based hybrid compatibilizer in reactive extrusion to yield compatibilized PP/PGA blends. It was observed that the domain size of PGA dispersed phased reduced with the incorporation of the hybrid compatibilizer. Further, the crystallization of PGA was fractionated at the crystallization temperature of PGA, and PP and co-crystallization of PP were suppressed for > 2 wt. % compatibilizer. With the increase in the hybrid compatibilizer, the toughness, strength, and thermal stability were improved, and the compatibilized blends showed more obvious shear thinning behavior at a lower shearing frequency, and lower complex viscosities and storage modulus at higher shearing frequency.[160]

Pandey et al. used microwave-assisted blends of PLLA and PGA to achieve enhanced compatibility in polar polymer blends. A 10% w/v solution of PLLA polymer was prepared in chloroform to which powdered PGA was suspended and irradiated at 260 W for 25 mins. It was observed that the 50/50 (w/w %) blends showed better compatibility. [161]

As PGA and PLA have similar structure and properties, it is expected that the strategies adopted to compatibilize PLA based blends can be used for PGA based blends and nanocomposites. For example, maleic anhydride grafted polyolefins can be used for compatibilisation of polar PLA or PGA with non-polar PE or PP.[162] Nuñez et al. used four different types of maleic anhydride grafted polymers,

View Article Online
DOI: 10.1039/D0GC01394C

namely styrene ethylene-butylene styrene rubber grafted maleic anhydride (SEBS-g-MA), metallocene polyethylene grafted maleic anhydride (PEm-g-MA) and two other PP grafted maleic anhydrides (PP1-g-MA and PP3-g-MA) for compatibilizing PLA and PP blends. The addition of the graft copolymers led to a decrease in coalescence rate and immobilization of the interface, thereby reduction of final particle size in the immiscible polymer system. The further added clay nanoparticles mainly localized in the PLA phase and compatibilized PP interface. This was due to the sequential addition of the blend components and the polar character of the interfaces (SEBS-g-MA and PP1-g-MA). PP1-g-MA was more efficient than SEBS-g-MA in terms of compatibilisation and thoughening.[163] Since clay layers can be used to enhance the gas/moisture barrier properties of polymers, such a strategy can be used for further enhancing the barrier properties of PGA based nanocomposites.

Nanoparticles like carbon nanotubes, silica, etc. can also be used to reduce the interfacial tension in polar and non-polar polymer blends. For instance, Lee et al. used 1~10 wt% of multiwalled carbon nanotubes (MWCNTs) to further compatibilize 50/50 (w/w) PLA and PP-g-MA blends. The MWCNTs localized in the PP phase and led to the finer dispersed morphology of PLA in the blends. The volume electrical resistivity of PLA/PP-g-MA blends dropped from ~10^{10} Ω cm to ~10^{5} Ω cm for 1 wt% MWCNTs composites while ~10 Ω cm for 10 wt% MWCNTs composites.[164] This strategy can be adopted to fabricate conductive polymer nanocomposites films of PGA. Apart from that, PLA/ MWCNT have shown potential in sensors to detect solvent leaks[165], such thin film composites of PGA can also be fabricated for precision sensors application. Yu et al. used hydrophobic silica nanoparticles to satisfactorily toughen and compatibilize PLA and thermoplastic polyurethane (TPU) elastomer. The silica nanoparticles localized at the interface of PLA and TPU, improving the interfacial adhesion via interaction. It had hydrophobic interaction with PLA while formed hydrogen bonds with TPU. 90/10 (w/w) PLA/TPU blend with 2 wt% SiO_2 exhibited high impact strength (~5 and 12.6 times that of the corresponding blend and PLA, respectively). [166] Such modifications can be attempted for flexible elastomeric blend composites in packaging applications.

Acrylic derivatives like glycidyl methacrylate (GMA) have also shown prominent results towards the compatibilization of polyester blend composites. Transesterification and epoxide ring-opening reactions are two mechanisms by which GMA interacts with other polymers.[167] Kim et al. used two different types of polyethylene modified GMA (PE-GMA, containing 8 wt% or 25 wt% GMA), and ethylene-acrylic copolymer (acrylic acid content was 9.54 %) to compatibilize PLA and low-density polyethylene blends. Coalescence was exceedingly suppressed with the addition of high GMA content PE-GMA, although copolymer of ethylene and acrylic acid was ineffective in compatibilization of the blends.[168] Kumar et al. used GMA as a reactive compatibilizer for PLA/PBAT blends. Dynamic mechanical analysis revealed an increase in the damping factor, confirming strong influence between PLA/PBAT blend in the presence of GMA. [90] Joncryl, a commercial derivative of 9 chain GMA, was used to compatibilize PLA/PBAT blends, where the compatibilized PLA/PBAT 80/20 (w/w) blends

View Article Online
DOI: 10.1039/D0GC01394C

showed higher viscosity and storage modulus than the unmodified blends. This increase was prominent at higher Joncryl concentration.[91] In another study, ethylene-methyl acrylate-glycidyl methacrylate copolymer (EMA-GMA) was used as a ternary blend component to toughen PLA/PBAT melt-processed blends. PLA/PBAT/EMA-GMA (75/10/15 wt%) blend exhibited a notched impact energy of 61.9 ± 2.7 kJ/m^2, ~13 times to that of PLA/PBAT (90/10) binary blends. The EMA-GMA was observed to wrap the PBAT particles and bridged the interface of PLA and PBAT.[169] Inspired from such approaches, PGA and other biodegradable polyester blends can be compatibilized for packaging film applications.

The progress of PGA and its nanocomposites towards different applications is currently in the cradle state of development. Based on its superiority compared to PLA in performance, different new potential applications of PGA can be envisioned. For instance, PLA has demonstrated its effectiveness in sensing[170, 171], electrical[172, 173], and thermal[174, 175] applications. Hydrophilic polymers and their blends are effective as antifouling surfaces in separation applications.[176, 177] In this regard, PLA based modified surfaces have demonstrated applications in photo-catalysis and oil-water separation applications.[178, 179] With a similar structure to PLA, PGA with higher crystallinity, higher strength and higher gas barrier properties, can be developed as alternatives to PLA in these different applications. Recently, electromagnetic interference (EMI) due to cross-talk between device signals is a growing concern in electronic devices.[180] Essentially conducting fillers along with magnetic nanoparticles are integrated into a polymer matrix to suppress electromagnetic interference. PLA based nanocomposites have shown effectiveness in such applications.[181, 182] The development of PGA and its composites is expected for high temperature and biodegradable EMI shielding applications.

Figure 11 pictographically illustrates possible groups of polymers that may be blended with PGA for targeting functional properties.

View Article Online
DOI: 10.1039/D0GC01394C

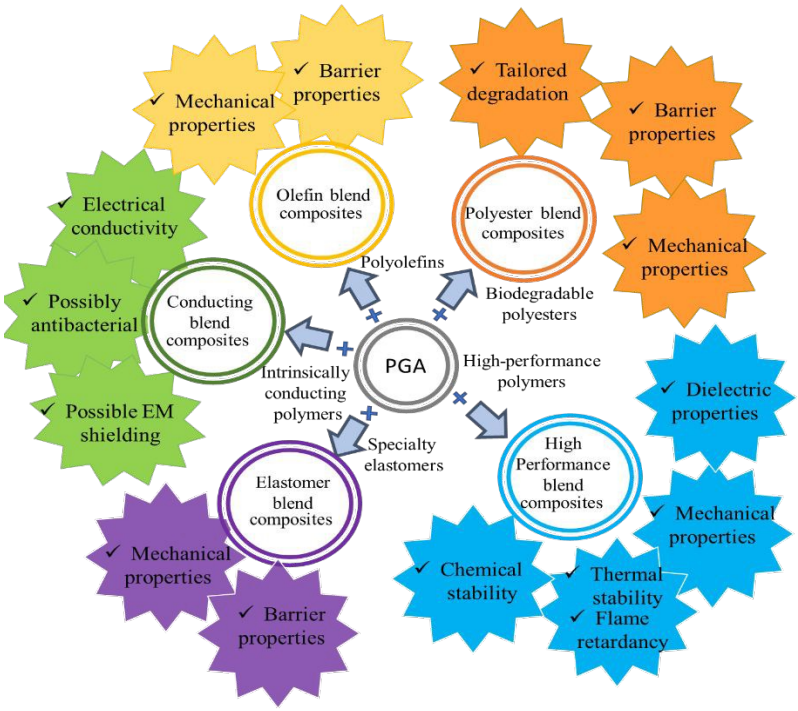

Figure 11: Anticipated enhancement of functional properties in PGA composites using polymer blending. Apart from the degradability of PGA, these blends may manifest specific characteristics utilizing the chemical and structural properties of the other blend component. (High-performance polymers, e.g., polyketones, polybenzoxazines, polysulphones, polyetherimides, polyphenylene sulfide, etc. Intrinsically conducting polymers, e.g., polyaniline, polypyrrole, polythiophene, poly(3,4-ethylenedioxythiophene)–poly (styrene sulfonate), etc. Specialty elastomer, e.g., thermoplastic polyurethane, rubbers, etc.) Note: For better EMI shielding capabilities, additional carbonaceous and/or magnetic nano-fillers may be required in tandem with the polymers.

6. Summary and outlook

Among the current biodegradable polymers, PGA has shown immense potentials by displaying unique properties including high resistance to common organic solvents, high heat distortion temperature, high gas barrier properties, high tensile strength, and stiffness alongside its relatively fast biodegradability and 100% compostability. However, it is still facing technical challenges and properties barriers prior to the large-scale production and application.

The monomer, glycolic acid, is currently predominantly produced from formaldehyde and carbon monoxide using acidic catalysts. Due to the lack of cheaper techniques to manufacture the monomer, the PGA production is still under extensive research. Kureha, in 2011 established its first plant in the USA with a capacity of 4,000 tonnes annually. In 2018, a Chinese company, Jiangsu Golden Polyalloy Material Co. Ltd., started a PGA plant with an annual capacity of 3,000 tonnes. For sustainable and strategic commercialization, Pujing Chemical Industry Co. Ltd is opening a 50,000 tonnes/year plant in 2020, which uses waste gas derived-CO from byproducts of the coal industry and converts these into

View Article Online
DOI: 10.1039/D0GC01394C

dimethyl oxalate following carbonization and esterification processes. This dimethyl oxalate is hydrogenated and used to produce PGA. This method is targeting the reduction of carbon emissions while being sustainable.

The sustainability of bioplastics can be quantified through CO_2 emissions and technical substitution potential, the later describes to what extent that petrochemical-based plastics can be substituted by bioplastics with similar properties, such as processing capacity at industry scale, mechanical robustness, thermal resistance, and stability. For future high-performance bioplastics to be reliably applied in engineering environments, biodegradable polymers are challenged to own high thermal and mechanical properties, chemical resistance, and good processability to compete with those well-developed engineering polymers. The examples for challenging applications are, but not limited to, high-temperature packaging for hot food, clothing, and electronics; devices that are difficult to access, such as in the deep ocean or oil field, which require the polymers to degrade after fulfilling their duties and leave no harmful debris to the environment.

The combination of high thermal stability, high gas barrier, and high mechanical strength of PGA makes it outstanding and competitive to PET, Nylon 6, or EVOH for packaging applications. Meanwhile, PGA can be processed via melt-extrusion, injection molding, blow-filming, and thermal forming, using standard polymer processing facilities.

The challenge lies in the melt processing window close to the thermal degradation temperature of PGA, and it is critical to choose appropriate processing temperatures and techniques to avoid degradation of the polymers and composites. The high processing temperature of PGA also challenges its melt-blending with biomass-based polymers such as starch and cellulose, as well as other commercial biopolymers such as PCL, PBS, and PHB. The hydrolysis rate of PGA can be tuned by orders of magnitude by copolymerization with PLA or by altering the end-group structure with hydrolysis stabilizers. The toughness and flexibility can be improved via copolymerization or blending. Modification of PGA using nanofillers such as natural clay, cellulose nanowhiskers, or other functional nanoparticles such as carbon nanotubes, graphene, and metal-organic frameworks are yet to be studied, which has the potential to generate high-performance biodegradable polymers for electrical, thermal, or optical devices.

Finally, it is essential to accelerate the use of biodegradable plastics instead of conventional single-use plastics. A circular economy is working on the principles of reducing, reuse, and recycle. It is imperative that public awareness through campaigns and presentations, as well as strict government regulations, impact the promotion of biodegradable plastics. With technological interventions, the production cost of degradable plastics and, in particular, PGA will go down. When reducing the impact of plastic waste pollution becomes our priority, the design and implementation of biodegradable polymers will help close the materials recycling loop and create a clean and sustainable environment.

Acknowledgments

A.L. and P.K.S. thank the funding support from Pujing Chemical Industry co. Ltd.

References:

1. R. Geyer, J. R. Jambeck and K. L. Law, *Science advances*, 2017, **3**, e1700782.
2. N. G. Shimpi, *Biodegradable and biocompatible polymer composites: Processing, properties and applications*, Woodhead Publishing, 2017.
3. F. Razza and F. D. Innocenti, *Asia - Pacific Journal of Chemical Engineering*, 2012, **7**, S301-S309.
4. J. H. Song, R. J. Murphy, R. Narayan and G. B. Davies, *Philos Trans R Soc Lond B Biol Sci*, 2009, **364**, 2127-2139.
5. R. G. Jones and U. i. d. c. p. e. a. P. Division, *Compendium of polymer terminology and nomenclature: IUPAC recommendations, 2008*, Royal Society of Chemistry Cambridge, 2009.
6. *Bioplastics Market Development Update*, European Bioplastics, Berlin, Germany, 2019.
7. B. T. K. Jim Jem, *Advanced Industrial and Engineering Polymer Research*, 2020, DOI: https://doi.org/10.1016/j.aiepr.2020.01.002.
8. K. Yamane, H. Sato, Y. Ichikawa, K. Sunagawa and Y. Shigaki, *Polymer Journal*, 2014, **46**, 769-775.
9. E. Göktürk, A. G. Pemba and S. A. Miller, *Polymer Chemistry*, 2015, **6**, 3918-3925.
10. E. de Jong, A. Higson, P. Walsh and M. Wellisch, *IEA Bioenergy, Task42 Biorefinery*, 2012, **34**.
11. M. A. M. Valderrama, R.-J. van Putten and G.-J. M. Gruter, *European Polymer Journal*, 2019.
12. K. J. Jem and B. Tan, *Advanced Industrial and Engineering Polymer Research*, 2020.
13. B.-Y. Yu, C.-Y. Chung and I.-L. Chien, *Computers & Chemical Engineering*, 2018, **119**, 85-100.
14. D. Gilding and A. Reed, *Polymer*, 1979, **20**, 1459-1464.
15. J. Nieuwenhuis, *Clinical materials*, 1992, **10**, 59-67.
16. Y. Lu, C. Schmidt and S. Beuermann, *Macromolecular Chemistry and Physics*, 2015, **216**, 395-399.
17. *United States Pat.*, 7,067,611, 2006.
18. C. Schmidt, M. Behl, A. Lendlein and S. Beuermann, *RSC advances*, 2014, **4**, 35099-35105.
19. D. Bratton, M. Brown and S. M. Howdle, *Chemical communications*, 2004, 808-809.
20. E. Gautier, P. Fuertes, P. Cassagnau, J. P. Pascault and E. Fleury, *Journal of Polymer Science Part A: Polymer Chemistry*, 2009, **47**, 1440-1449.
21. World patent WO03/006525, 2003.
22. V. M. Kemo, C. Schmidt, Y. Zhang and S. Beuermann, *Macromolecular Chemistry and Physics*, 2016, **217**, 842-849.
23. O. Dechy-Cabaret, B. Martin-Vaca and D. Bourissou, *Chemical reviews*, 2004, **104**, 6147-6176.
24. V. Singh and M. Tiwari, *International Journal of Polymer Science*, 2010, **2010**.
25. M. Ayyoob, D. H. Lee, J. H. Kim, S. W. Nam and Y. J. Kim, *Fibers and Polymers*, 2017, **18**, 407-415.
26. V. Sanko, I. Sahin, U. A. Sezer and S. Sezer, *Polymer Journal*, 2019, **51**, 637-647.
27. K. Schwarz and M. Epple, *Macromolecular Chemistry and Physics*, 1999, **200**, 2221-2229.
28. K. Takahashi, I. Taniguchi, M. Miyamoto and Y. Kimura, *Polymer*, 2000, **41**, 8725-8728.
29. H. Sato, F. Kobayashi, Y. Kawakami, K. Yamane, Y. Amano and T. Sato, *Journal*, 2014.
30. J. C. Middleton and A. J. Tipton, *Biomaterials*, 2000, **21**, 2335-2346.
31. C. Chu, in *Biotextiles as Medical Implants*, Elsevier, 2013, pp. 275-334.
32. X. S. Wu and N. Wang, *Journal of Biomaterials Science, Polymer Edition*, 2001, **12**, 21-34.

33. J. Li, S. N. Rothstein, S. R. Little, H. M. Edenborn and T. Y. Meyer, *Journal of the American Chemical Society*, 2012, **134**, 16352-16359.
34. M. Tracy, K. Ward, L. Firouzabadian, Y. Wang, N. Dong, R. Qian and Y. Zhang, *Biomaterials*, 1999, **20**, 1057-1062.
35. N. Wang, X. S. Wu, C. Li and M. F. Feng, *Journal of Biomaterials Science, Polymer Edition*, 2000, **11**, 301-318.
36. S. H. Lee, B. S. Kim, S. H. Kim, S. W. Choi, S. I. Jeong, I. K. Kwon, S. W. Kang, J. Nikolovski, D. J. Mooney and Y. K. Han, *Journal of Biomedical Materials Research Part A: An Official Journal of The Society for Biomaterials, The Japanese Society for Biomaterials, and The Australian Society for Biomaterials and the Korean Society for Biomaterials*, 2003, **66**, 29-37.
37. R. S. Bezwada, D. D. Jamiolkowski, I.-Y. Lee, V. Agarwal, J. Persivale, S. Trenka-Benthin, M. Erneta, J. Suryadevara, A. Yang and S. Liu, *Biomaterials*, 1995, **16**, 1141-1148.
38. Q. Cai, J. Bei and S. Wang, *Polymer*, 2002, **43**, 3585-3591.
39. D. Pappalardo, T. r. Mathisen and A. Finne-Wistrand, *Biomacromolecules*, 2019, **20**, 1465-1477.
40. R. Zurita, L. Franco, J. Puiggalí and A. Rodríguez-Galán, *Polymer degradation and stability*, 2007, **92**, 975-985.
41. P. Dobrzynski, J. Kasperczyk, H. Janeczek and M. Bero, *Macromolecules*, 2001, **34**, 5090-5098.
42. K. Avgoustakis, *Encyclopedia of biomaterials and biomedical engineering*, 2005, **1**, 1-11.
43. Y. Liu, X. Bai and A. Liang, *International Journal of Polymer Science*, 2016, **2016**.
44. L. Wang, Z. Zhang, H. Chen, S. Zhang and C. Xiong, *Journal of Polymer Research*, 2010, **17**, 77.
45. Y. Jung, S.-H. Lee, S.-H. Kim, J. C. Lim and S. H. Kim, *Journal of Biomaterials Science, Polymer Edition*, 2013, **24**, 386-397.
46. R. Zurita, J. Puiggalí, L. Franco and A. Rodríguez‐Galán, *Journal of Polymer Science Part A: Polymer Chemistry*, 2006, **44**, 993-1013.
47. E. Díaz-Celorio, L. Franco, A. Rodríguez-Galán and J. Puiggalí, *Polymer degradation and stability*, 2013, **98**, 133-143.
48. Q. Cai, J. Bei and S. Wang, *Journal of Biomaterials Science, Polymer Edition*, 2000, **11**, 273-288.
49. S. H. Choi and T. G. Park, *Journal of Biomaterials Science, Polymer Edition*, 2002, **13**, 1163-1173.
50. C. Min, W. Cui, J. Bei and S. Wang, *Polymers for Advanced Technologies*, 2005, **16**, 608-615.
51. A. Smola, P. Dobrzynski, M. Cristea, J. Kasperczyk, M. Sobota, K. Gebarowska and H. Janeczek, *Polymer Chemistry*, 2014, **5**, 2442-2452.
52. X. Chen, X. Wu, Z. Fan, Q. Zhao and Q. Liu, *Polymers for Advanced Technologies*, 2018, **29**, 1684-1696.
53. E. Zini, M. Scandola, P. Dobrzynski, J. Kasperczyk and M. Bero, *Biomacromolecules*, 2007, **8**, 3661-3667.
54. W. Xiaomeng, C. Xiaoyu and F. Zhongyong, *European Polymer Journal*, 2018, **101**, 140-150.
55. S. Wen, Y. Li, W. Chen, Y. Lei, C. Luo and Y. Hou, *Applied Organometallic Chemistry*, 2018, **32**, e4177.
56. S. Davachi, B. Kaffashi and J. M. Roushandeh, *Polymers for Advanced Technologies*, 2012, **23**, 565-573.
57. H. R. Kricheldorf, T. Mang and J. M. Jonté, *Die Makromolekulare Chemie: Macromolecular Chemistry and Physics*, 1985, **186**, 955-976.
58. H. Fukuzaki, M. Yoshida, M. Asano, M. Kumakura, T. Mashimo, H. Yuasa, K. Imai, H. Yamanaka, U. Kawaharada and K. Suzuki, *Journal of biomedical materials research*, 1991, **25**, 315-328.
59. H. Fukuzaki, M. Yoshida, M. Asano, Y. Aiba and M. Kumakura, *European polymer journal*, 1990, **26**, 457-461.

60. A. Nakayama, N. Kawasaki, S. Aiba, Y. Maeda, I. Arvanitoyannis and N. Yamamoto, *Polymer*, 1998, **39**, 1213-1222.
61. X. Liu, M. Hong, L. Falivene, L. Cavallo and E. Y.-X. Chen, *Macromolecules*, 2019, **52**, 4570-4578.
62. A. Pedna, L. Rosi, M. Frediani and P. Frediani, *Journal of Applied Polymer Science*, 2015, **132**.
63. A. Buchard, D. R. Carbery, M. G. Davidson, P. K. Ivanova, B. J. Jeffery, G. I. Kociok‐Köhn and J. P. Lowe, *Angewandte Chemie International Edition*, 2014, **53**, 13858-13861.
64. H. Nakajima, K. Loos, S. Ishizu and Y. Kimura, *Macromolecular rapid communications*, 2018, **39**, 1700865.
65. Y. Wang, Z. Jia, J. Jiang, X. Mao, X. Pan and J. Wu, *Macromolecules*, 2019, **52**, 7564-7571.
66. A. G. Amador, A. Watts, A. E. Neitzel and M. A. Hillmyer, *Macromolecules*, 2019, **52**, 2371-2383.
67. M. Soccio, N. Lotti, L. Finelli, M. Gazzano and A. Munari, *Journal of Polymer Science Part B: Polymer Physics*, 2010, **48**, 1901-1910.
68. Y. Reyhanoglu, E. Sahmetlioglu and E. Gokturk, *ACS Sustainable Chemistry & Engineering*, 2019, **7**, 5103-5110.
69. F. Jing, M. R. Smith and G. L. Baker, *Macromolecules*, 2007, **40**, 9304-9312.
70. X. Jiang, E. B. Vogel, M. R. Smith and G. L. Baker, *Macromolecules*, 2008, **41**, 1937-1944.
71. Y. Chatani, K. Suehiro, Y. Ôkita, H. Tadokoro and K. Chujo, *Die Makromolekulare Chemie: Macromolecular Chemistry and Physics*, 1968, **113**, 215-229.
72. C. Nakafuku and H. Yoshimura, *Polymer*, 2004, **45**, 3583-3585.
73. F. Nishimura, H. Hoshina, Y. Ozaki and H. Sato, *Polymer Journal*, 2019, **51**, 237-245.
74. H. Sato, M. Miyada, S. Yamamoto, K. R. Reddy and Y. Ozaki, *RSC advances*, 2016, **6**, 16817-16823.
75. J. E. Báez and Á. Marcos-Fernández, *International Journal of Polymer Analysis and Characterization*, 2015, **20**, 637-644.
76. S. Lee, C. Hongo and T. Nishino, *Macromolecules*, 2017, **50**, 5074-5079.
77. L. W. McKeen, *Permeability properties of plastics and elastomers*, William Andrew, 2016.
78. Y. B. Tee, R. A. Talib, K. Abdan, N. L. Chin, R. K. Basha and K. F. M. Yunos, *BioResources*, 2016, **11**, 1518-1540.
79. C. Calvino, N. Macke, R. Kato and S. J. Rowan, *Progress in Polymer Science*, 2020, 101221.
80. I. U. Unalan, C. Wan, Ł. Figiel, R. T. Olsson, S. Trabattoni and S. Farris, *Nanotechnology*, 2015, **26**, 275703.
81. S. Merritt, A. M. Wemyss, S. Farris, S. Patole, G. Patias, D. M. Haddleton, B. Shollock and C. Wan, *ACS Applied Polymer Materials*, 2020.
82. D. Plackett and I. Siró, in *Multifunctional and nanoreinforced polymers for food packaging*, Elsevier, 2011, pp. 498-526.
83. S.-G. Hong, H.-W. Hsu and M.-T. Ye, *Journal of thermal analysis and calorimetry*, 2013, **111**, 1243-1250.
84. G.-X. Chen, H.-S. Kim, E.-S. Kim and J.-S. Yoon, *Polymer*, 2005, **46**, 11829-11836.
85. I.-N. Georgousopoulou, S. Vouyiouka, P. Dole and C. D. Papaspyrides, *Polymer degradation and stability*, 2016, **128**, 182-192.
86. K. J. Jem, J. F. van der Pol and S. de Vos, in *Plastics from bacteria*, Springer, 2010, pp. 323-346.
87. L. Liao, C. Zhang and S. Gong, *European polymer journal*, 2007, **43**, 4289-4296.
88. Y. Song, M. Kamphuis, Z. Zhang, L. T. Sterk, I. Vermes, A. Poot, J. Feijen and D. Grijpma, *Acta biomaterialia*, 2010, **6**, 1269-1277.
89. S. Kennouche, N. Le Moigne, M. Kaci, J.-C. Quantin, A.-S. Caro-Bretelle, C. Delaite and J.-M. Lopez-Cuesta, *European Polymer Journal*, 2016, **75**, 142-162.
90. M. Kumar, S. Mohanty, S. K. Nayak and M. Rahail Parvaiz, *Bioresour Technol*, 2010, **101**, 8406-8415.

91. R. Al-Itry, K. Lamnawar and A. Maazouz, *Polymer Degradation and Stability*, 2012, **97**, 1898-1914.
92. S. S. Ray and M. Bousmina, *Polymer*, 2005, **46**, 12430-12439.
93. H. Ye, K. Zhang, D. Kai, Z. Li and X. J. Loh, *Chem Soc Rev*, 2018, **47**, 4545-4580.
94. H. Janke, J. Bohlin, R. Lomme, S. Mihaila, J. Hilborn, W. Feitz and E. Oosterwijk, *Acta biomaterialia*, 2017, **59**, 234-242.
95. P. E. Keller and R. T. Kouzes, *Water vapor permeation in plastics*, Pacific Northwest National Lab.(PNNL), Richland, WA (United States), 2017.
96. D. K. Platt, *Biodegradable polymers: market report*, iSmithers Rapra Publishing, 2006.
97. J. Guillet, H. Huber and J. Scott, *the Royal Society of Chemistry, Cambridge*, 1992.
98. L. S. Nair and C. T. Laurencin, *Progress in polymer science*, 2007, **32**, 762-798.
99. P. A. Gunatillake and R. Adhikari, *Eur Cell Mater*, 2003, **5**, 1-16; discussion 16.
100. J. A. Tamada and R. Langer, *Proc Natl Acad Sci U S A*, 1993, **90**, 552-556.
101. L. N. Woodard and M. A. Grunlan, *ACS Macro Letters*, 2018, **7**, 976-982.
102. S. Bonhomme, A. Cuer, A. Delort, J. Lemaire, M. Sancelme and G. Scott, *Polymer degradation and Stability*, 2003, **81**, 441-452.
103. C. Dussud and J.-F. Ghiglione, presented in part at the CIESM Workshop Monogr, 2014.
104. S. Shawe, F. Buchanan, E. Harkin-Jones and D. Farrar, *Journal of materials science*, 2006, **41**, 4832-4838.
105. X. Hu, G. Hu, K. Crawford and C. B. Gorman, *Journal of Polymer Science Part A: Polymer Chemistry*, 2013, **51**, 4643-4649.
106. A. Vieira, J. Vieira, R. Guedes and A. Marques, *Materials science forum*, 2010, **636**, 825-832.
107. L. I. S. de la Cruz, F. J. M. Rodríguez, C. Velasco-Santos, A. Martínez-Hernández and M. Gutiérrez-Sánchez, *Journal of Polymer Research*, 2016, **23**, 113.
108. F. Rouhollahi, S. A. Hosseini, F. Alihosseini, A. Allafchian and F. Haghighat, *Fibers and Polymers*, 2018, **19**, 2056-2065.
109. S. S. Spearman, F. Irin, S. Ramesh, I. V. Rivero, M. J. Green and O. L. Harrysson, *International Journal of Polymeric Materials and Polymeric Biomaterials*, 2019, **68**, 360-367.
110. A. Z. I. Pereira, M. C. Delpech, F. G. da Costa and F. B. da Cruz, *Journal of Applied Polymer Science*, 2016, **133**.
111. J. Yekrang, D. Semnani, A. Z. Seyghalani and S. Razavi, *Indian Journal of Fibre & Textile Research (IJFTR)*, 2017, **42**, 264-270.
112. X. Lin, W. Wang, W. Zhang, Z. Zhang, G. Zhou, Y. Cao and W. Liu, *Tissue Eng Part C Methods*, 2017, **23**, 86-97.
113. S. Toosi, H. Naderi-Meshkin, F. Kalalinia, H. HosseinKhani, A. Heirani-Tabasi, S. Havakhah, S. Nekooei, A. H. Jafarian, F. Rezaie and M. T. Peivandi, *Journal of Materials Science: Materials in Medicine*, 2019, **30**, 33.
114. S. Liu, G. Wu, X. Zhang, J. Yu, M. Liu, Y. Zhang, P. Wang and X. Yin, *Fibers and Polymers*, 2019, **20**, 229-235.
115. S. Fu, D. Yang and P. Zhang, *The Journal of The Textile Institute*, 2019, **110**, 1580-1587.
116. J. Takeuchi, H. Suzuki, M. Murata, Y. Kakei, S. Ri, M. Umeda and T. Komori, *J Oral Maxillofac Surg*, 2013, **71**, e126-131.
117. C. S. Nabzdyk, M. Chun, S. G. Pathan, D. W. Nelson, J.-O. You, M. D. Phaneuf, F. W. LoGerfo and L. Pradhan-Nabzdyk, *Journal of Nanomaterials*, 2015, **2015**.
118. A. Agarwal and N. D. Gupta, *Quintessence International*, 2012, **43**.
119. J. B. Jonnalagadda and I. V. Rivero, *Journal of the mechanical behavior of biomedical materials*, 2014, **40**, 33-41.
120. R. M. Allaf, I. V. Rivero and I. N. Ivanov, *Journal of Applied Polymer Science*, 2015, **132**.
121. B. N. Kim, Y.-G. Ko, T. Yeo, E. J. Kim, O. K. Kwon and O. H. Kwon, *ACS Biomaterials Science & Engineering*, 2019, **5**, 5266-5272.

122. H. Fujimaki, K. Uchida, G. Inoue, O. Matsushita, N. Nemoto, M. Miyagi, K. Inage, S. Takano, S. Orita, S. Ohtori, K. Tanaka, H. Sekiguchi and M. Takaso, *J Biomed Mater Res B Appl Biomater*, 2020, **108**, 326-332.
123. I. Keridou, L. Franco, P. Turon, L. J. del Valle and J. Puiggalí, *Macromolecular Materials and Engineering*, 2018, **303**, 1800100.
124. N. Dehnavi, K. Parivar, V. Goodarzi, A. Salimi and M. R. Nourani, *Polymers for Advanced Technologies*, 2019, **30**, 2192-2206.
125. Y. Song, M. Ren, Y. Wu, S. Li, C. Song, F. Wang and Y. Huang, *RSC advances*, 2019, **9**, 20174-20184.
126. B. Weber, R. Schoenauer, F. Papadopulos, P. Modregger, S. Peter, M. Stampanoni, A. Mauri, E. Mazza, J. Gorelik and I. Agarkova, *Biomaterials*, 2011, **32**, 9630-9641.
127. K. B. Lee, K. R. Yoon, S. I. Woo and I. S. Choi, *J Pharm Sci*, 2003, **92**, 933-937.
128. T. Yamanaka, Y. Sawai and H. Hosoi, *Otolaryngol Head Neck Surg*, 2013, **149**, 342-344.
129. T. Kuwata, S. Shinohara, M. Takenaka, S. Oka, Y. Chikaishi, A. Hirai, K. Kuroda, T. So and F. Tanaka, *Gen Thorac Cardiovasc Surg*, 2016, **64**, 558-560.
130. M. Fujita, Y. Kinoshita, E. Sato, H. Maeda, S. Ozono, H. Negishi, T. Kawase, Y. Hiraoka, T. Takamoto, Y. Tabata and Y. Kameyama, *Tissue Eng*, 2005, **11**, 1346-1355.
131. E. D. Boland, T. A. Telemeco, D. G. Simpson, G. E. Wnek and G. L. Bowlin, *J Biomed Mater Res B Appl Biomater*, 2004, **71**, 144-152.
132. S. Morita, T. Takagi, R. Abe, H. Tsujimoto, Y. Ozamoto, H. Torii and A. Hagiwara, *Biomed Res Int*, 2018, **2018**, 4515949.
133. R. D. Boehm, J. Daniels, S. Stafslien, A. Nasir, J. Lefebvre and R. J. Narayan, *Biointerphases*, 2015, **10**, 011004.
134. R. D. Boehm, P. Jaipan, S. A. Skoog, S. Stafslien, L. VanderWal and R. J. Narayan, *Biointerphases*, 2016, **11**, 011008.
135. N. Ashammakhi, E. A. Makela, K. Vihtonen, P. Rokkanen, H. Kuisma and P. Tormala, *Biomaterials*, 1995, **16**, 135-138.
136. N. Ashammakhi, E. A. Mäkelä, P. Törmälä, T. Waris and P. Rokkanen, *European Journal of Plastic Surgery*, 2000, **23**, 423-428.
137. *United States Pat.,* 10/375,719, 2004.
138. N. Tariq, S. Tayyaba, M. W. Ashraf, G. Sarwar and M. F. Wasim, presented in part at the 2016 2nd International Conference on Robotics and Artificial Intelligence (ICRAI), 2016.
139. *United States Pat.,* 7,153,265, 2006.
140. *United States Pat.,* 11/123,497, 2005.
141. *United States Pat.,* 11/887,333, 2011.
142. *United States Pat.,* 8,399,077, 2013.
143. J. Vartiainen, Y. Shen, T. Kaljunen, T. Malm, M. Vähä‐Nissi, M. Putkonen and A. Harlin, *Journal of Applied Polymer Science*, 2016, **133**.
144. N. Ibrišimović, M. Ibrišimović, M. Barth and U. Bohrn, *Monatshefte für Chemie-Chemical Monthly*, 2010, **141**, 125-130.
145. E. Fortunati, S. Mattioli, L. Visai, M. Imbriani, J. L. Fierro, J. M. Kenny and I. Armentano, *Biomacromolecules*, 2013, **14**, 626-636.
146. C. Gomes, R. G. Moreira and E. Castell-Perez, *J Food Sci*, 2011, **76**, N16-24.
147. M. Esfandyari-Manesh, Z. Ghaedi, M. Asemi, M. Khanavi, A. Manayi, H. Jamalifar, F. Atyabi and R. Dinarvand, *journal of pharmacy research*, 2013, **7**, 290-295.
148. R. C. Correia, A. F. Jozala, K. F. Martins, T. C. V. Penna, E. A. de Rezende Duek, C. de Oliveira Rangel-Yagui and A. M. Lopes, *World Journal of Microbiology and Biotechnology*, 2015, **31**, 649-659.
149. Z. Ghalanbor, M. Korber and R. Bodmeier, *Pharm Res*, 2010, **27**, 371-379.
150. L. E. Hill, T. M. Taylor and C. Gomes, *J Food Sci*, 2013, **78**, N626-632.

151. E. Walejewska, J. Idaszek, M. Heljak, A. Chlanda, E. Choinska, V. Hasirci and W. Swieszkowski, *Polymer Degradation and Stability*, 2020, **171**, 109030.
152. K. Samadi, M. Francisco, S. Hegde, C. A. Diaz, T. A. Trabold, E. M. Dell and C. L. Lewis, *Polymer Degradation and Stability*, 2019, **170**, 109018.
153. A. K. Biswal and S. Saha, *Journal of Applied Polymer Science*, 2019, **136**, 48009.
154. A. K. Biswal and S. Saha, *J Colloid Interface Sci*, 2020, **566**, 120-134.
155. H. Hu, R. Zhang, J. Wang, W. B. Ying, L. Shi, C. Yao, Z. Kong, K. Wang and J. Zhu, *Green Chemistry*, 2019, **21**, 3013-3022.
156. M. Kemme and R. Heinzel-Wieland, *J Funct Biomater*, 2018, **9**, 4.
157. G. Gorrasi, A. Meduri, P. Rizzarelli, S. Carroccio, G. Curcuruto, C. Pellecchia and D. Pappalardo, *Reactive and Functional Polymers*, 2016, **109**, 70-78.
158. W. Sikorska, G. Adamus, P. Dobrzynski, M. Libera, P. Rychter, I. Krucinska, A. Komisarczyk, M. Cristea and M. Kowalczuk, *Polymer degradation and stability*, 2014, **110**, 518-528.
159. T. M. Madkour, S. A. Salem and S. A. Miller, *Physical Chemistry Chemical Physics*, 2013, **15**, 5982-5991.
160. H. Yang, Z. Cai, H. Liu, Z. Cao, Y. Xia, W. Ma, F. Gong, G. Tao and C. Liu, *Journal of Polymer Science*, 2020.
161. A. Pandey, G. C. Pandey and P. B. Aswath, *Journal of the mechanical behavior of biomedical materials*, 2008, **1**, 227-233.
162. S. Pivsa-Art, J. Kord-Sa-Ard, W. Pivsa-Art, R. Wongpajan, N. O-Charoen, S. Pavasupree and H. Hamada, *Energy Procedia*, 2016, **89**, 353-360.
163. K. Nuñez, C. Rosales, R. Perera, N. Villarreal and J. Pastor, *Polymer bulletin*, 2011, **67**, 1991-2016.
164. T.-W. Lee and Y. G. Jeong, *Composites science and technology*, 2014, **103**, 78-84.
165. K. Kobashi, T. Villmow, T. Andres, L. Häußler and P. Pötschke, *Smart materials and structures*, 2009, **18**, 035008.
166. F. Yu and H.-X. Huang, *Polymer Testing*, 2015, **45**, 107-113.
167. A. V. Reis, A. R. Fajardo, I. T. Schuquel, M. R. Guilherme, G. J. Vidotti, A. F. Rubira and E. C. Muniz, *The Journal of organic chemistry*, 2009, **74**, 3750-3757.
168. Y. F. Kim, C. N. Choi, Y. D. Kim, K. Y. Lee and M. S. Lee, *Fibers and Polymers*, 2004, **5**, 270-274.
169. N. Wu and H. Zhang, *Materials Letters*, 2017, **192**, 17-20.
170. K. Kobashi, T. Villmow, T. Andres and P. Pötschke, *Sensors and Actuators B: Chemical*, 2008, **134**, 787-795.
171. K. Li, K. Dai, X. Xu, G. Zheng, C. Liu, J. Chen and C. Shen, *Colloid and Polymer Science*, 2013, **291**, 2871-2878.
172. D. Wu, Q. Lv, S. Feng, J. Chen, Y. Chen, Y. Qiu and X. Yao, *Carbon*, 2015, **95**, 380-387.
173. S. Lebedev, O. Gefle, E. Amitov, D. Y. Berchuk and D. Zhuravlev, *Polymer Testing*, 2017, **58**, 241-248.
174. A. Ameli, D. Jahani, M. Nofar, P. Jung and C. Park, *Composites Science and Technology*, 2014, **90**, 88-95.
175. P. Gong, S. Zhai, R. Lee, C. Zhao, P. Buahom, G. Li and C. B. Park, *Industrial & Engineering Chemistry Research*, 2018, **57**, 5464-5471.
176. P. K. Samantaray, G. Madras and S. Bose, *Advanced Sustainable Systems*, 2019, 1900017.
177. B. Boruah, P. K. Samantaray, G. Madras, J. M. Modak and S. Bose, *Chemical Engineering Journal*, 2020, 124777.
178. X. Hou, Y. Cai, M. Mushtaq, X. Song, Q. Yang, F. Huang and Q. Wei, *Journal of nanoscience and nanotechnology*, 2018, **18**, 5617-5623.
179. J. Shi, L. Zhang, P. Xiao, Y. Huang, P. Chen, X. Wang, J. Gu, J. Zhang and T. Chen, *ACS Sustainable Chemistry & Engineering*, 2018, **6**, 2445-2452.
180. A. V. Menon, B. Choudhury, G. Madras and S. Bose, *Chemical Engineering Journal*, 2020, **382**, 122816.

181. K. Zhang, H.-O. Yu, K.-X. Yu, Y. Gao, M. Wang, J. Li and S. Guo, *Composites Science and Technology*, 2018, **156**, 136-143.
182. F. Ren, Z. Li, L. Xu, Z. Sun, P. Ren, D. Yan and Z. Li, *Composites Part B: Engineering*, 2018, **155**, 405-413.

View Article Online
DOI: 10.1039/D0GC01394C